AD A030855

FG

REPORT NO. FAA-RD-76-124

(12)

MEASUREMENTS OF AIRCRAFT XENON STROBE LIGHT CHARACTERISTICS

Charles O. Phillips, Jr.

U.S. DEPARTMENT OF TRANSPORTATION
Transportation Systems Center
Kendall Square
Cambridge MA 02142

AUGUST 1976
FINAL REPORT

Prepared for

U.S. DEPARTMENT OF TRANSPORTATION
FEDERAL AVIATION ADMINISTRATION
Systems Research and Development Service
Washington DC 20591

TECHNICAL REPORT STANDARD TITLE PAGE

1. Report No. FAA-RD-76-124	2. Government Accession No.	3. Recipient's Catalog No.
4. Title and Subtitle MEASUREMENTS OF AIRCRAFT XENON STROBE LIGHT CHARACTERISTICS		5. Report Date Aug[illegible]976
		6. Performing Organization Code
7. Author(s) Charles O. Phillips, Jr		8. Performing Organization Report No. [illegible]-TSC-FAA-75-15
9. Performing Organization Name and Address U.S. Department of Transportation Transportation Systems Center Kendall Square Cambridge MA 02142		10. Work Unit No. FA514/R6055T
		11. Contract or Grant No.
		13. Type of Report and Period Covered Final Report, 1970-1974
12. Sponsoring Agency Name and Address U.S. Department of Transportation Federal Aviation Administration Systems Research and Development Service Washington DC 20591		14. Sponsoring Agency Code
15. Supplementary Notes		

16. Abstract

This report provides data on the characteristics of aircraft xenon str[illegible]ights related to their potential for use as the cooperati[illegible]ment in Optical IR (Infrared) Airborne Proximity Warning In[illegible]tor (APWI) systems. It includes a description of pertinent cha[illegible]istics, measurements of radiation geometry and power output of [illegible]cted strobes, a discussion of environmental effects including lamp aging, variation in supply voltage, thermal and installation effects. Detailed measurements of spectral peak radiant intensity in addition to spectral radiant energy are presented along with measurements of rise time, duration, and fall time as a function of wave length.

17. Key Words	18. Distribution Statement
Aircraft Exterior Lighting Xenon Strobe Light Light Measurement	DOCUMENT IS AVAILABLE TO THE PUBLIC THROUGH THE NATIONAL TECHNICAL INFORMATION SERVICE, SPRINGFIELD, VIRGINIA 22161

19. Security Classif. (of this report)	20. Security Classif. (of this page)	21. No. of Pages	22. Price
Unclassified	Unclassified	80	

Form DOT F 1700.7 (8-69)

404 082

PREFACE

This report is part of a Federal Aviation Administration program of visual collision avoidance including Airborne Proximity Warning Indicator (APWI). This part of the program was performed by the Transportation Systems Center (TSC) at Cambridge, Massachusetts. The contents of the report are a summary of two reports prepared for TSC: (1) "A Survey of Aircraft Strobe Characteristics" by Juri Valge and Susan Hunt, Charles Stark Draper Laboratory of the Massachusetts Institute of Technology, Report R-706, November 1971; and (2) "Report on Aircraft Strobe Lamp Measurements," by F. C. Allard, Naval Underwater Systems Center, Special Forces Department, Report SA31-67-72, October 1972 and January 1973.

METRIC CONVERSION FACTORS

Approximate Conversions to Metric Measures

Symbol	When You Know	Multiply by	To Find	Symbol
		LENGTH		
in	inches	2.5	centimeters	cm
ft	feet	30	centimeters	cm
yd	yards	0.9	meters	m
mi	miles	1.6	kilometers	km
		AREA		
in^2	square inches	6.5	square centimeters	cm^2
ft^2	square feet	0.09	square meters	m^2
yd^2	square yards	0.8	square meters	m^2
mi^2	square miles	2.6	square kilometers	km^2
	acres	0.4	hectares	ha
		MASS (weight)		
oz	ounces	28	grams	g
lb	pounds	0.45	kilograms	kg
	short tons (2000 lb)	0.9	tonnes	t
		VOLUME		
tsp	teaspoons	5	milliliters	ml
Tbsp	tablespoons	15	milliliters	ml
fl oz	fluid ounces	30	milliliters	ml
c	cups	0.24	liters	l
pt	pints	0.47	liters	l
qt	quarts	0.95	liters	l
gal	gallons	3.8	liters	l
ft^3	cubic feet	0.03	cubic meters	m^3
yd^3	cubic yards	0.76	cubic meters	m^3
		TEMPERATURE (exact)		
°F	Fahrenheit temperature	5/9 (after subtracting 32)	Celsius temperature	°C

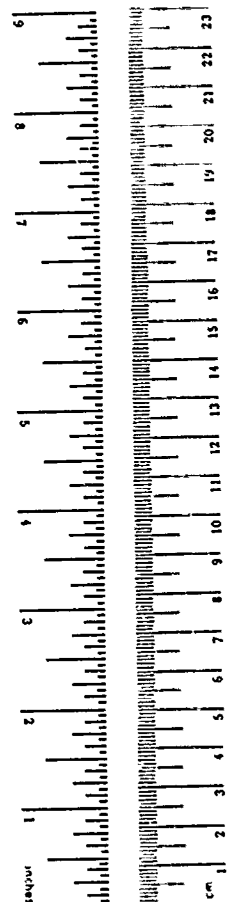

Approximate Conversions from Metric Measures

Symbol	When You Know	Multiply by	To Find	Symbol
		LENGTH		
mm	millimeters	0.04	inches	in
cm	centimeters	0.4	inches	in
m	meters	3.3	feet	ft
m	meters	1.1	yards	yd
km	kilometers	0.6	miles	mi
		AREA		
cm^2	square centimeters	0.16	square inches	in^2
m^2	square meters	1.2	square yards	yd^2
km^2	square kilometers	0.4	square miles	mi^2
ha	hectares (10,000 m^2)	2.5	acres	
		MASS (weight)		
g	grams	0.035	ounces	oz
kg	kilograms	2.2	pounds	lb
t	tonnes (1000 kg)	1.1	short tons	
		VOLUME		
ml	milliliters	0.03	fluid ounces	fl oz
l	liters	2.1	pints	pt
l	liters	1.06	quarts	qt
l	liters	0.26	gallons	gal
m^3	cubic meters	35	cubic feet	ft^3
m^3	cubic meters	1.3	cubic yards	yd^3
		TEMPERATURE (exact)		
°C	Celsius temperature	9/5 (then add 32)	Fahrenheit temperature	°F

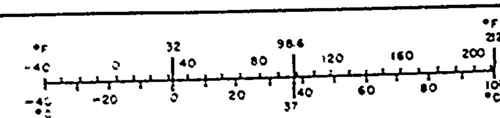

TABLE OF CONTENTS

LIST OF ILLUSTRATIONS

LIST OF ILLUSTRATIONS (CONTINUED)

LIST OF TABLES

1. INTRODUCTION

1.1 BACKGROUND

This report on Measurements of Aircraft Xenon Strobe Light Characteristics has been performed by the Transportation Systems Center (TSC) as part of the Federal Aviation Administration program of visual collision avoidance including Airborne Proximity Warning Indicator (APWI). It is a summary of two reports prepared for TSC by (a) the Charles Stark Draper Laboratory of the Massachusetts Institute of Technology, Report R-706, "A Survey of Aircraft Strobe Characteristics" by Juri Valge and Susan Hunt, November 1971; and (b) the Naval Underwater Systems Center, Report SA31-67-72, "Report on Aircraft Strobe Lamp Measurements" in two parts by F.C. Allard, Special Forces Department, 16 October 1972 and January 1973.

1.2 PURPOSE

The purpose of this report is to provide data on the characteristics of xenon strobe lights related to their proposed use as the cooperative element in Optical IR (infrared) Airborne Proximity Warning Indicator (APWI) systems. It is not intended to draw conclusions on the suitability of such strobe lights for that purpose. Such conclusions must include, in addition, data characterizing APWI detector performance and atmospheric transmission, as well as further data on the statistical variation of the intensity of strobe lights in operational use.

1.3 REMARKS

Aircraft exterior lights fall into the following categories:

1. Landing Lights
2. Position Lights
3. Riding Lights (water operation)
4. Anticollision Lights
5. Supplemental Lights

The first four categories fall under the Federal Aviation Regulations (FAR) Airworthiness Standards for Fixed Wing Aircraft and Rotorcraft Parts 23, 25, 27, and 29, in the installation of which angular coverage, color, and intensity are specified according to their purpose.

The anticollision light regulation calls for a red flashing light with a minimum effective intensity of 100 candelas. This requirement has been met by both the rotating beacon and the xenon strobe light. Many users found, however, that a clear lens, particularly for the xenon strobe, increased the conspicuity over the red lens for the same input power. A number of users acquired white strobe lights of the same or lower input power as supplemental lights, in addition to or in place of the anticollision lights.

As a result, an amendment, 91-90, effective August 11, 1971, was adopted permitting the use of either red or white anticollision light systems. In addition, it (1) expanded the chromaticity-coordinate range for aviation white; (2) increased the minimum effective intensities from 100 to 400 candelas; (3) required that all aircraft certified for night flight carry an anticollision light by August 11, 1972.

The increase in minimum effective intensity by a factor of 4 is assumed to be accomplished without an increase in input power by changing from a red to clear lens. Users still desiring a red lens will need a redesigned higher power unit to make up for the attenuation of the red lens in the visual portion of the spectrum. A controversy exists over this requirement from the standpoint of increased cost, increased power required from small aircraft, and the decrease in uniformity of radiated power between red and white xenon strobe units in the infrared portion of the spectrum.

Independent of the development of anticollision lights for visual collision avoidance, an optical infrared Airborne Proximity Warning Indicator (APWI) approach was developed in which the cooperative element is a xenon strobe light. Infrared sensitive (0.8 to 1.1 μ) silicon detectors sense the proximity of a xenon strobe carried by an intruding aircraft, produce a signal that alerts the pilot audibly and indicates bearing to the intruder, to improve his visual detection.

The same xenon strobe units that meet the requirements for anticollision lights are believed to provide, under most conditions, sufficient radiation in the near infrared for adequate detection between 1 and 3 nautical miles (Ref. 5). Rotating beacon anticollision lights do not generate sufficient instantaneous radiation in the near infrared and are not considered for this application.

Because these xenon strobe units have been commercially developed, only to meet the anticollision regulations defined in the visual region of the spectrum, inadequate information is available to evaluate their use for the Optical Infrared APWI application. This report is intended to provide additional data for that purpose.

1.4 SCOPE

As mentioned in 1.1, this report is a summary of two studies on xenon strobe lights, performed by MIT Draper Laboratory and the Naval Underwater System Center (NUSC). The latter study was implemented to augment the measurements accomplished by MIT. For this reason, there is some redundancy in the measurement of the anticollision strobe units performed by both organizations. Basically, Sections 3 and 4 include the work accomplished by MIT on a wide selection of xenon strobe units for aircraft exterior lighting. whereas Section 5 include the work accomplished by NUSC on three anticollision strobe units.

2. DESCRIPTION OF AIRCRAFT XENON STROBE CHARACTERISTICS

2.1 BASIC XENON STROBE UNIT DESCRIPTION

The basic xenon strobe unit meeting the anticollision light requirement consists of the components shown in Figure 2-1. Direct current input power at 14 or 24 volts and an average of 50 watts are applied to a DC to DC converter charge unit that converts the

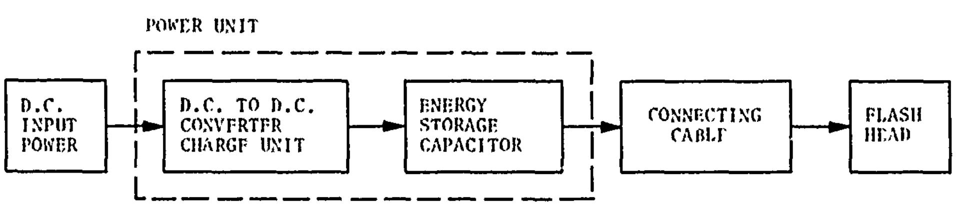

Figure 2-1. Basic Xenon Strobe Components

input voltage to approximately 400 to 500 volts, charging the capacitor to a stored energy of approximately 20 joules or watt seconds. At a rate of approximately once per second, the stored energy is discharged through a connecting cable to the flash head containing the trigger, and the xenon-filled flash lamp emitting a peak radiated power of approximately 4,000 watts per steradian, from 350 to 1250 nanometers.

Table 2-1 indicates the electrical characteristics of four selected strobe units.

The following description depicts the characteristics of the radiated output for different units and different conditions of operation.

TABLE 2-1. ELECTRICAL CHARACTERISTICS OF AIRCRAFT STROBES

Ref. No.	Characteristic	Bullock #1	Grimes #3	S.D.I #7	Whelen #3
(1)	Peak input power (P_L) (watts) to power supply	50	63.6	47.6	56.0
(2)	Total energy (E_p) input to the strobe power supply (watt-sec/pulse)	51	50.8	38.3	40
(3)	Total energy input (E_L) to flash lamp (watt-second/pulse)	16.6	19.6	25.2	22
(4)	Peak lamp current (amps)	120	281	187.5	200
(5)	Lamp resistance (ohms)	2.52	1.77	1.45	1.70

2.2 VISUAL CHARACTERISTICS

The xenon strobe has been used so far in high speed photography (see Reference 3) and stroboscopy primarily to take advantage of its short duration light pulse of "freeze motion." Its utility in aircraft exterior lighting is mainly in conserved electrical input power for a given physiological, psychological or electro-optical effect. Depending upon the power level received by the eye, there are two opposite effects. The enhancement of sensory effects is discussed on the basis of research performed 60 to 80 years ago, in the work of Broca and Sulzer, while at threshold levels some degradation was observed by Blondel and Rey.

Broca and Sulzer studied the effects of pulse duration and intensity on the net stimulus. Blondel and Rey studied the effects of pulse duration on the threshold of perception. They arrived at an empirical formula for the power available from a pulse, for the threshold detection case:

$$\phi_e = \frac{\int_{t_1}^{t_2} \phi(t)\,dt}{0.2 + \left(t_2 - t_1\right)} \qquad (2\text{-}1)$$

where

ϕ = effective intensity of received radiation, i.e., intensity produced by an equivalent source with a duration of 3 or more seconds. (The effects of atmospheric attenuation are not considered.)

$\phi(t)$ = instantaneous intensity of received radiation.

t = time; subscripts refer to integration limits.

If the path attenuation effects are included, then

$$E = \frac{\int_{t_1}^{t_2} \phi(t) K_e \left(\lambda_1 t_1 r_1 o\right) dt}{0.2 + \left(t_2 - t_1\right)} \qquad (2\text{-}2)$$

It should be observed again that Equation 2-1, which is a conclusion made by Blondel and Rey in 1911, considers the threshold value of flashed light perception, where the shortest duration of a light pulse was one millisecond, and the pulse shape half-sinusoidal. Aircraft strobes have durations which vary from 75 to 600 microseconds.

If the pulse amplitude is above the threshold level, an actual enhancement of eye sensitivity takes place, and the perceived light pulse provides a visual stimulus equal to 5 times the steady value of the same light level. Again, these conclusions were made with much longer duration light pulses than 600 microseconds and with a spectral source of a different energy distribution. Therefore, the properties of human eye response to an aircraft strobe pulse, in the above duration range, must be established and, if a maximum condition for detection exists, it must be regulated as the acceptable pulse length.

2.3 OPTICAL IR STROBE CHARACTERISTICS

In contrast to visual detection which is dependent on integrated intensity or energy content of the light pulse, the chosen electro-optical detection process is dependent on the instantaneous peak power radiated.

The following parameters characterize the performance of strobe lamps in relation to optical IR APWI detection. Peak Power Radiated is related to:

(a) Spectral distribution (wavelength)

(b) Temporal distribution (pulse shape, repetition rate, age)

(c) Spacial distribution (beam pattern)

These parameters are affected by

a. Unit Characteristics:

1. Lens (red or clear, configuration)
2. Reflector (configuration)
3. Strobe lamp (conversion efficiency, configuration)
4. Cable length (resistance, inductance)
5. Energy Storage (capacitance, resistance, inductance, voltage)
6. Charge circuit (conversion efficiency, regulation)

b. Mounting Characteristics:

1. Number and distribution of units
2. Location by aircraft type as related to obstructions and reflections

c. Environmental Characteristics:

1. Temperature
2. Dust
3. Turbulence affecting aircraft attitude

d. Operational Characteristics:

1. Turns and banks affecting aircraft attitude
2. Ascent and descent affecting aircraft attitude

The remainder of this report provides data on the interrelationships of some of these parameters.

3. MEASUREMENTS OF THE RADIATION GEOMETRY AND POWER OUTPUT OF SELECTED STROBES

3.1 PROCUREMENT OF STROBES

Aircraft strobes for various mounting positions and locations on the vehicle were obtained from the following companies:

a. Bullock Magnetics Co.

b. J.F. Davy Co.

c. Grimes Manufacturing Co.

d. Symbolic Displays, Inc.

e. Whelen Engineering Co.

f. INTAIRCO, Inc. (SENIT)

Aircraft strobes were also acquired from the Honeywell Company, Aerospace Division, but no measurements are available. No aircraft strobes were obtained from the Aeroflash Corporation.

3.2 TEST PROCEDURE FOR RADIATION GEOMETRY

After physical inspection, cleaning and assignment of a 0° reference direction, the lamp to be tested and its power supply were mounted on a small rotary table, inside a large pyramidal light trap (see Figure 3-1). The detector, its power supply and an oscilloscope with a camera, were set up approximately 114 feet away from the strobe. The horizontal plane is defined as the plane which contains the roll and pitch axes of an aircraft, if the lamp is mounted in its designated position (see Figure 3-2).

The choice of the 0° point in the horizontal plane was arbitrary. However, all similar type lamps from the same manufacturer were assigned the same 0° reference point. (For example, all Whelen lamps which have Fresnel lens type covers are at 0°, when the lamp tube anode faces an observer stationed at the sensor.)

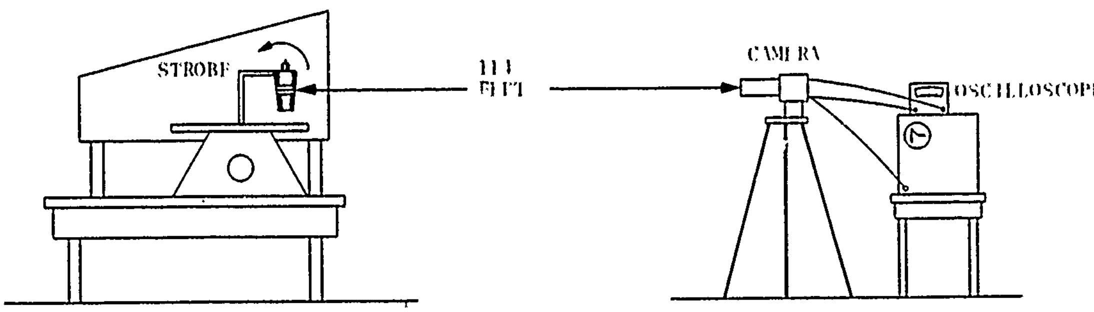

Figure 3-1. Physical Strobe Light Test Setup

In every case, with the lamp upright in the test fixture, 90° counter-clockwise rotation of the lamp from a horizontal plane presented a 90° lamp position to the sensor. (See Figures 3-3 and 3-4.)

Each lamp had a 1/2-hour warmup and settling-in period before test data were taken. The DC power for the individual lamp supplies came from a regulated power supply which was checked at the start of the 1/2-hour warmup, then, at the beginning of the test, and finally, at the end of the test period. The lamps were operated at the voltages stated on their respective power supplies, i.e., either 14 or 28 VDC.

Detector outputs were recorded for the following two cases:

a. Lamp upright (vertical)

0° Horizontal angle and the vertical angle inserted at -5°, -10°, -15°, -20°, -25°, -30°, -45°, -60°, -75°, -90°.

The same vertical angles were used for measurements at 90°, 180°, and 270° horizontal angles.

b. <u>Lamp inverted in the holder</u>

0° horizontal angle, and the vertical angle inserted at +5°, +10°, +15°, +20°, +25°, +30°, +45°, +50°, +75°, +90°.

Again, the same vertical angles were used for horizontal angles of 90°, 180°, and 270°.

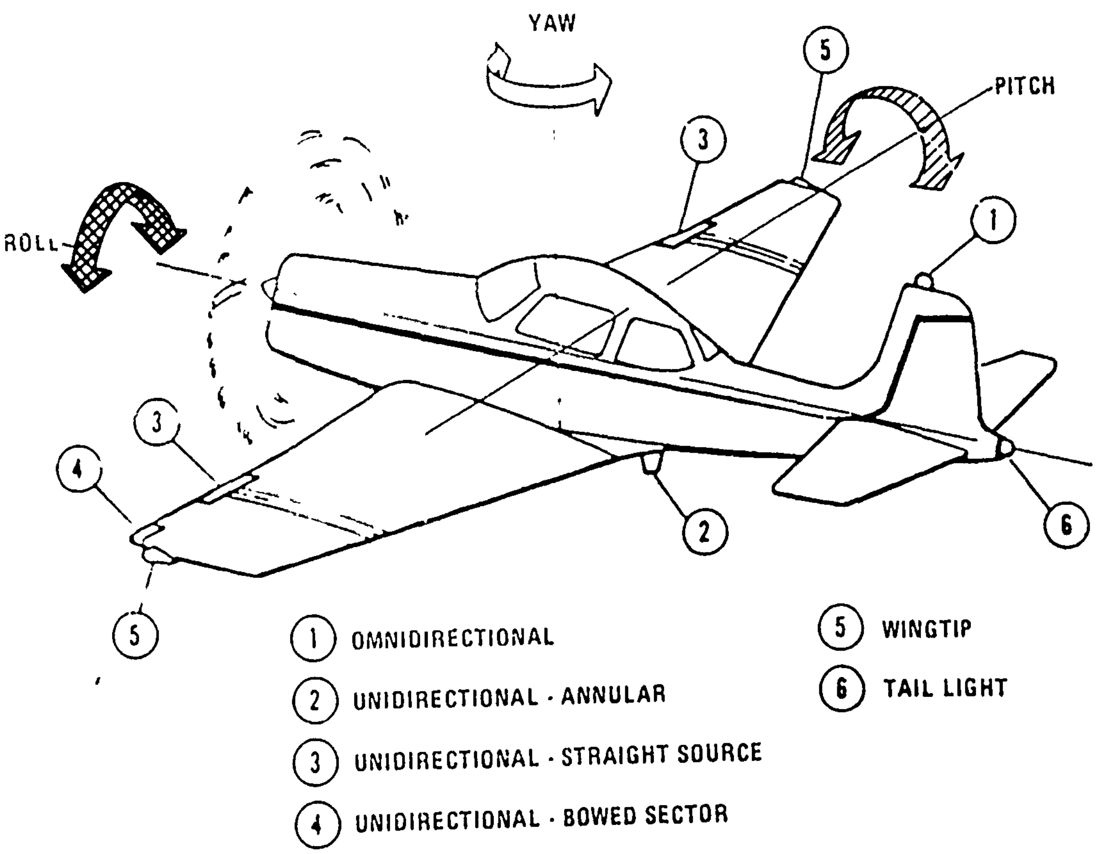

Figure 3-2. Typical Locations of Xenon Strobes Aboard an Aircraft

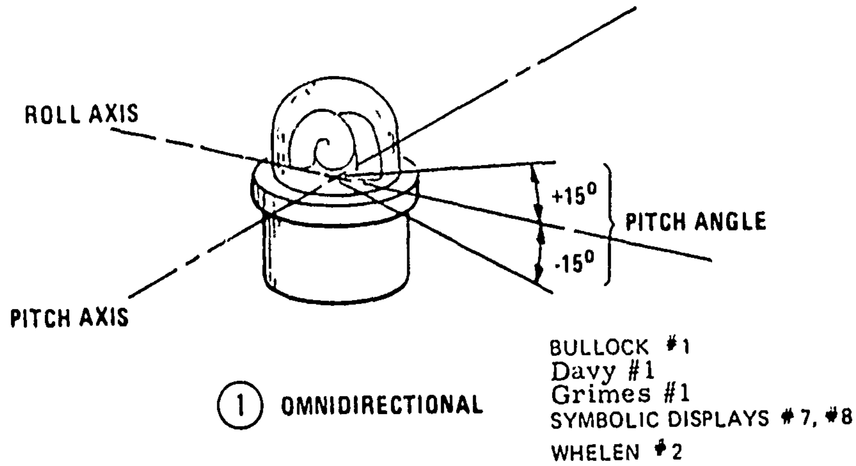

Figure 3-3. Omnidirectional Strobe Lamp with Optical Cover

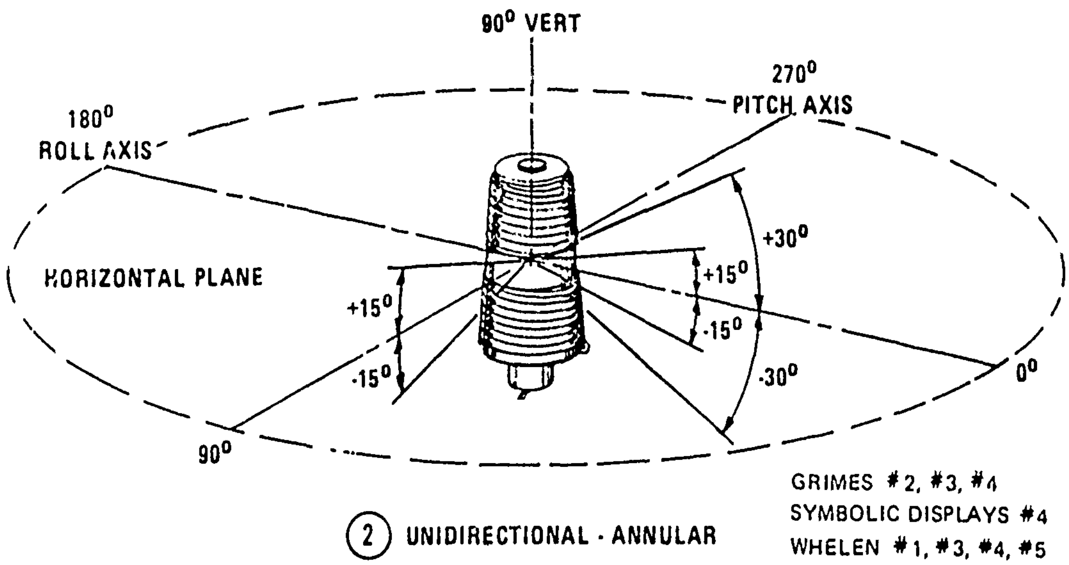

Figure 3-4. Unidirectional Strobe Lamp with Optical Cover

The power in watts/steradian was calculated for each position, and normalized to the maximum power found in all angular positions tested. It should be noted that the power in watts/steradian expresses the lamp power output within the 8.7×10^{-4}-radian field of view used for testing the power level at each of the positions required according to the Work Statement. Power levels for the lamps tested are listed in Table 3-1.

3.3 STROBE LAMP AND HOUSING TYPES

Figure 3-2 is a sketch of an aircraft which has samples of all the lamp types under test installed on the air frame. While it is unlikely that an airplane would carry all the lights shown, the figure simplifies the explanation of lamp types according to their mounting positions.

The flash lamp tube shape is illustrated in Figure 3-3, and influences the radiation pattern. However, the radiation pattern is much more severely affected by the reflectors and optics of the transparent covers. Therefore, the lamps which do not have an optically shaped housing can be designated as omnidirectional. They have hemispherical envelopes and seem to radiate unimpeded in hemispherical directions, according to physical characteristics of the flash tube shape. A large number of lamps have optical beam shaping attained by built-in reflectors and special optically shaped envelopes. These lamps are here designated as unidirectional. They have been designed in a way that sends most of the luminous output in a particular direction. Such output orientation can be attained by an optical lens arrangement of the strobe cover, as in the case of the Whelen strobes which produce radiation output in a 360° horizontal sector.

A parabolic reflector is placed behind the xenon flash tube for some of the Grimes and Symbolic Displays. These lamps then send out light into specific sectors. The "sector" lamps are typified by straight or somewhat bowed tubes backed by reflectors which follow the xenon lamp shape and direct the radiation into a beam in the desired direction. Figures 3-4, 3-5 and 3-6 show the envelope shapes encountered.

The power in watts/steradian was calculated for each position, and normalized to the maximum power found in all angular positions tested. It should be noted that the power in watts/steradian expresses the lamp power output within the 8.7×10^{-4}-radian field of view used for testing the power level at each of the positions required according to the Work Statement. Power levels for the lamps tested are listed in Table 3-1.

3.3 STROBE LAMP AND HOUSING TYPES

Figure 3-2 is a sketch of an aircraft which has samples of all the lamp types under test installed on the air frame. While it is unlikely that an airplane would carry all the lights shown, the figure simplifies the explanation of lamp types according to their mounting positions.

The flash lamp tube shape is illustrated in Figure 3-3, and influences the radiation pattern. However, the radiation pattern is much more severely affected by the reflectors and optics of the transparent covers. Therefore, the lamps which do not have an optically shaped housing can be designated as omnidirectional. They have hemispherical envelopes and seem to radiate unimpeded in hemispherical directions, according to physical characteristics of the flash tube shape. A large number of lamps have optical beam shaping attained by built-in reflectors and special optically shaped envelopes. These lamps are here designated as unidirectional. They have been designed in a way that sends most of the luminous output in a particular direction. Such output orientation can be attained by an optical lens arrangement of the strobe cover, as in the case of the Whelen strobes which produce radiation output in a 360° horizontal sector.

A parabolic reflector is placed behind the xenon flash tube for some of the Grimes and Symbolic Displays. These lamps then send out light into specific sectors. The "sector" lamps are typified by straight or somewhat bowed tubes backed by reflectors which follow the xenon lamp shape and direct the radiation into a beam in the desired direction. Figures 3-4, 3-5 and 3-6 show the envelope shapes encountered.

TABLE 3-1. SELECTED STROBE CHARACTERISTICS (Continued)

Make/Model	Pulse			Peak Output w/SR	Angle of Max. Power	Lamp-to-P.S. Cable Length	Type
	Rise Time µsec	Duration µsec	Repetition Rate PPM				
S.D.I. #4 30-0021	40	250	47	835	10°	3-ft.	Unidirectional Annular
S.D.I. #5 30-0005A	60	350	47	1043	90°	3-ft.	Tail
S.D.I. #6 30-002	60	240	47	1015	50°	3-ft.	Wing Tip
Symbolic Display #7 30-0001	33 33	265 265	46 46	1045 990	45° 45°	3-ft. 3-ft.	Clear, Omnidir. Red, Omnidirectional
S.D.I. #8 67-2018 Self-Contained P.S.	39	275	46	1001 910	45° 45°	6-inch 6-inch	Clear, Omnidir. Red, Omnidirectional
S.D.I. #9 30-0187-21	29	176	41	7327	0°	3-ft.	Unidirectional Bowed

TABLE 3-1. SELECTED STROBE CHARACTERISTICS (Continued)

Make/Model	Pulse			Peak Output w/SR	Angle of Max. Power	Lamp-to-P.S. Cable Length	Type
	Rise Time μsec	Duration μsec	Repetition Rate PPM				
Whelen #1 HR28-R28	20	210	41	2431	0°	6-inch	Unidirectional Annular
Whelen #2 SA28-A28	28	210	52	1352	45°	6-inch	Omnidirectional
Whelen #3-#3 HS28-528	70 26	300 210	43 43	1325 2370	0° 0°	30-ft. 6-inch	Unidirectional Annular
Whelen #4-#8 HA28	70 26	300 210	43 43	1580 2260	0° 0°	30-ft. 6-inch	Clear Lens, Unidirectional Annular
Whelen #5-#7 HS28	70 26	330 200	43 43	1438 2360	0° 0°	30-ft. 6-inch	Red Lens, Unidirectional Annular
Whelen #10 A429	35	310	41	745	45°	30-ft.	Wing Tip
Whelen #11 A430	48	410	43	670	85°	30-ft.	Tail
SENIT Type 5727	76 msec	100 msec	71 RPM	18	---	------	Rotating Beacon

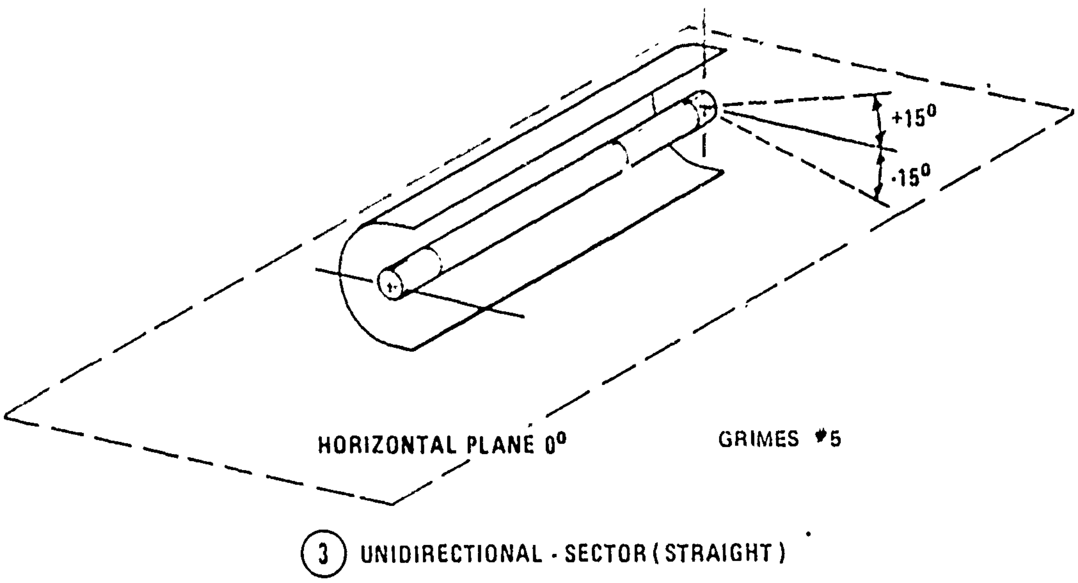

Figure 3-5. Straight Unidirectional Strobe Lamp

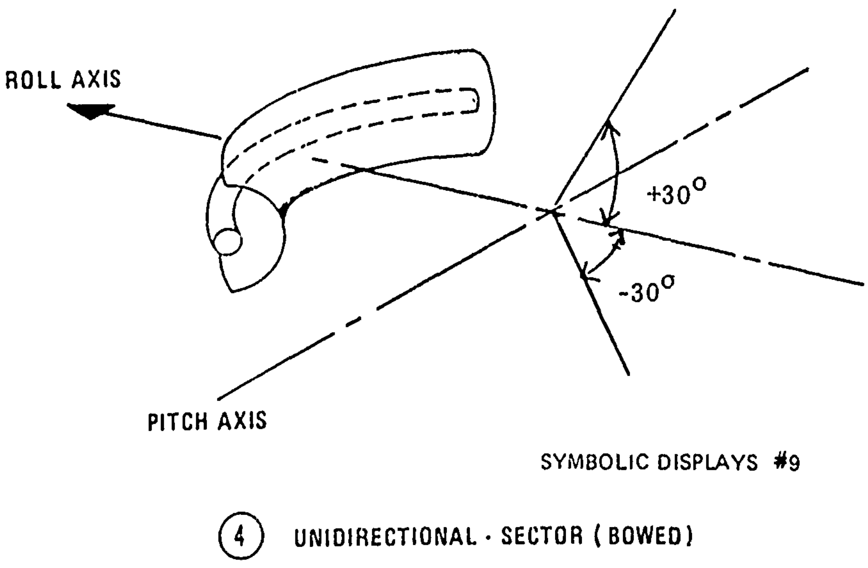

Figure 3-6. Bowed Unidirectional Strobe Lamp

Finally, there are some strobe lamps intended for use on either the wingtips or the extreme rear of the fuselage or top of the rudder. These are small lamps, contained in stremlined housings as shown in Figures 3-7 and 3-8. Their radiation is directed by the housing and airframe blockage into sectors, as apparent from Figures 3-2, 3-7 and 3-8.

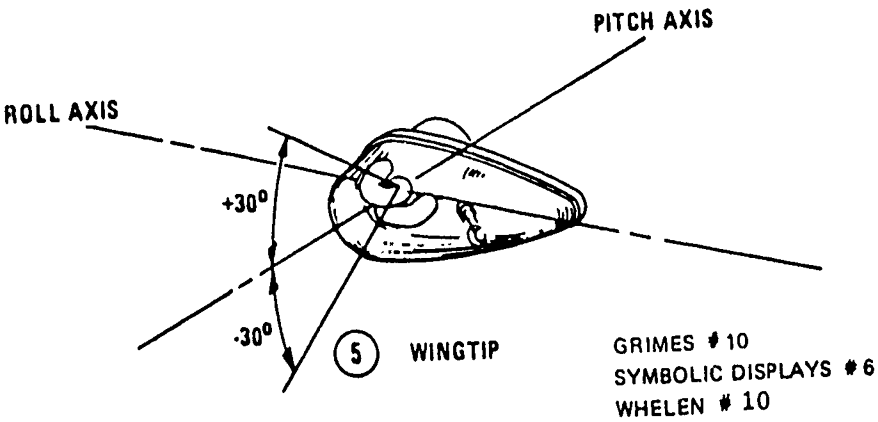

Figure 3-7. Wingtip Strobe Lamp

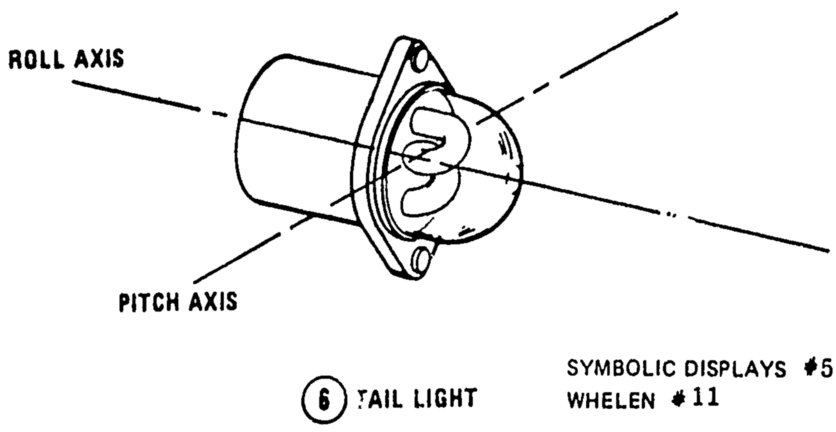

Figure 3-8. Typical Tail Light Strobe Lamp

4. ENVIRONMENTAL EFFECTS ON SELECTED STROBE

4.1 GENERAL FACTORS

The aircraft strobe may be subjected to a wide range of temperature conditions depending upon the climate, operating altitude, and the location of the strobe on the aircraft. The environmental changes considered here mainly cosist of temperature and vibration. Vibration is likely to cause some type of catastrophic failure, rather than change the output characteristics of the lamps. Besides the meteorological environment changes, the factors which affect lamp output are age and the input voltage level to the power supply.

4.2 LAMP AGING

Several lamps were subjected to 8-hour-a-day operation, to determine their peak power endurance. All these lamps used regulated DC input power and were housed in similar enclosures. The results are listed in Table 4-1. Besides the lamps examined for aging during this contract, another lamp was tested for output power after 2640 hours of operation, but, unfortunately, no knowledge of the input power is available.

4.3 SUPPLY VOLTAGE EFFECTS

The DC voltage applied to the lamp power supplies is critical as viewed from two aspects:

a. Optical lamp output energy depends upon the DC level and,

b. Aircraft power supply is not limitless and overloading may occur.

While the question of aircraft power generation system capability is discussed elsewhere, the effects upon output energy are given in Table 4-2.

TABLE 4-1. CHANGES OF STROBE OUTPUT POWER WITH OPERATING TIME

Manufacturer	Operating Hours	Peak Power Change
Bullock	140	40%
Grimes	60	20%
SDI	130	50%
Whelen #4	138	33%
#6	138	17%
#7	138	4%
Whelen - DOT/TSC*	2640	?

*The DOT/TSC personnel had installed a Whelen lamp HS-28 with a clear lens on the State Street Bank Building in Boston. This lamp was removed from its installation and turned over to Draper Laboratory for testing. The lamp had run for 2640 hours continuously. At Draper Laboratory, the lamp was operated for 45 minutes and then its power output was found to be 903 watts/steradian in the APWI detector range.

TABLE 4-2. CHANGES OF STROBE OUTPUT POWER WITH VARIATION OF RATE SUPPLY VOLTAGE

Percent Rated Supply Voltage	30 ft. Power Supply Cable; Percent Power Output of Power at Rated Input Voltage	0.75 ft. Power Supply Cable; Percent Power Output of Power at Rated Input Voltage
73.5	45.8	58.8
78.5	60.0	67.9
85.8	74.6	76.1
89.3	91.3	----
92.7	74.6	89.4
96.4	97.5	----
100	100	100
103.6	104	----
107.1	111	115
113.2	114.2	114.5

4.4 THERMAL EFFECTS

At first, the lamps themselves were subjected to thermal cycling, and no changes in characteristics were noted. Then the lamp power supplies were subjected to fast and slow thermal cycling and the relative output power was monitored. The fast cycling indicated that there was considerable time lag in the appearance of thermal effects, as shown in Table 4-3. When longer periods were used in cooling the lamp power supply at various temperatures, the effects were more noticeable; they are listed in Tables 4-4 and 4-5.

4.5 INSTALLATION EFFECTS

The problems of cable length and lamp-to-aircraft geometry are not strictly environmental effects, but are presented here as effects which now cause variations not controlled by any rules. These effects are listed in Table 4-6.

TABLE 4-3. RAPID THERMAL CYCLING

Temperature °F	Percent Change in Output Compared to Initial at 70°F		
	Lamp #1	Lamp #2	Lamp #3
70	100	100	100
+120	100	97.6	97.6
-30	97.4	95.5	91.6
+120	98.6	97.6	91.6
-30	97.4	81.8	89.5
+120	96.0	93.1	89.5
-30	91.9	93.1	85.4
70	100	93.1	83.3

TABLE 4-4. SLOW THERMAL CYCLING OF LAMP POWER SUPPLIES*

Temperature °F	Percent of Original Pulse Rate at 70°F		Percent Output Energy	
	Lamp #1	Lamp #2	Lamp #1	Lamp #2
70	100	100	100	100
30	100	92.8	100	79
0	100	90.5	100	65.8
-20	100	95.3	100	52.6
-40	100	97.5	124	36.8

*The lamps under test were operated for two minutes at each temperature tabulated until the chamber reached a temperature of -40°F. Then the strobe power supplies were disconnected from the DC power line and left at -40°F for 5 minutes. After this, the DC power was again applied to the power supplies and the strobe output and repetition rate recorded.

TABLE 4-5. OPERATION OF STROBE POWER SUPPLIES AT -40°F

Time After Turn-On, Minutes	Percent Pulse Rate of Original Rate at 70°F		Percent of Output Energy at 70°F	
	Lamp #1	Lamp #2	Lamp #1	Lamp #2
2	*	150	*	21
10	*	128	*	21.1
15	100**	109	88.9**	26.3

*Lamp did not flash.

**A double power supply was used, and the lamp was attached to the other half of the power supply after failing to operate when plugged into the first half.

TABLE 4-6. VARIATIONS IN THE CHARACTERISTICS DUE TO INSTALLATION*

Electrical Characteristics	Changes by a Factor of
Peak Power	0.5 to 0.7
Rise Time	2 to 3
Pulse Duration	1.1 to 1.5

*Mechanical and optical variations depend on the extent the mounting space geometry permits changes in lamp radiation plane and direction.

5. ANTICOLLISION LIGHT MEASUREMENTS

5.1 TEST SCOPE

This section is concerned with measurements of three types of aircraft strobes meeting the requirements of the Anticollision Light FAR. They are:

1. Whelen Strobe, Model HD, Units #1 and #7L.
2. Grimes Strobe, Part No. 30-0504-1, Unit #3 (clear lens).
3. Symbolic Displays Strobe, Hoskins Silvar Star #1 (clear lens) Part No. 700801.

The Whelen and Grimes strobe Units #1 and #3, respectively, were discussed in the previous sections. The Whelen #7L strobe was used during the Optical IR, PWI flight tests and had accumulated a significant number of operations prior to the measurement. The Hoskins Silvar Star #1 was acquired at the end of the measurement program and was measured separately from the other units.

The measurements are intended to supplement previously obtained data, including the following:

a. Spectral peak radiant intensity

b. Spectral radiant energy

c. Rise time, duration and decay time vs. wavelength

d. Spectral analysis from 0 to 200 kilohertz

e. Radiation geometry (beam patterns)

f. Photometric calculations

g. Strobe stability

Briefly, lamp radiation was measured with two detector systems. A grating-type spectroradiometer with an S-1 photomultiplier was used to obtain spectral resolution of 5 nm from 350 to 800 nm and

10 nm from 700 to 1250 nm. Broad band spectral measurements were made with a silicon photodiode having a measurable response from 400 to 1100 nm (nominal). With a DOT-supplied filter, the response of the latter device was limited to a range from 750 to 1100 nm (nominal). Readout of both devices was via oscilliscope, supplemented by CRT photographs.

Separation of flashlamp and detector was typically 1m or 3m depending on sensitivity vs. bandwidth considerations. As a check on the applicability of the data to lamp output a. much greater ranges, lamp output was measured at $\sqrt{2}$ range steps from 0.68m to 42.87m with a small area detector (0.051 cm^2). Detector output was found to follow the $1/R^2$ law reasonably well at all ranges employed.

In order to obtain the absolute measurements following, the spectroradiometer was calibrated with a 1000-watt standard of spectral irradiance. This standard, designated QM-66, was supplied to NUSC by the National Bureau of Standards (NBS), assuring - by virture of its being a secondary standard - an accurate calibration of the spectroradiometer. The silicon photodiode was not recalibrated, since it was employed only for relative measurements.

The radiometric axis for the bulk of the strobe lamp measurements was contained in the plane parallel to the lamp mounting plate, and passing through the center of the lamp. A 0^o elevation angle was obtained, in accordance with the definitions of MIT CSDL Report R-706. The azimuthal angle for the radiometric axis was determined in accordance with scribe marks on the lamp bases, as supplied, or, in the case of the Grimes lamps, in accordance with the convention established in the privious sections.

5.2 SPECTRAL PEAK RADIANT INTENSITY

The spectral distribution of radiant flux in the output of three selected types of strobes was measured in the following manner:

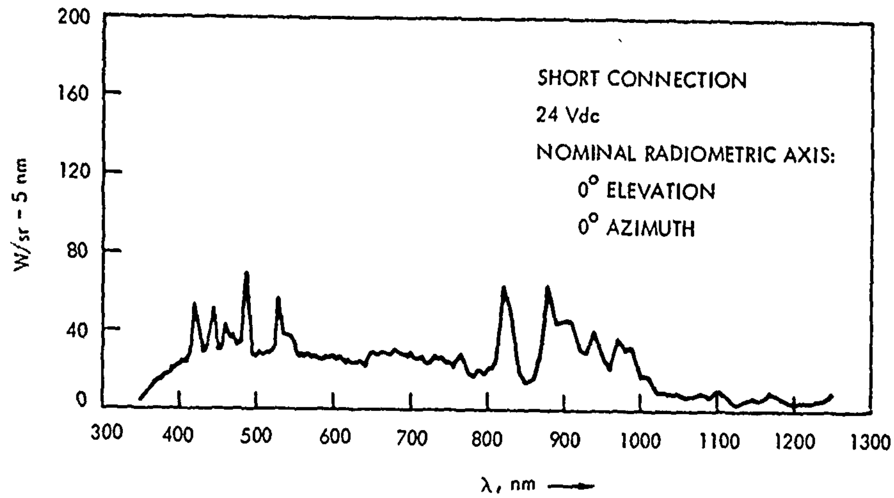

Figure 5-1. Spectral Peak Intensity of Whelen Strobe 1

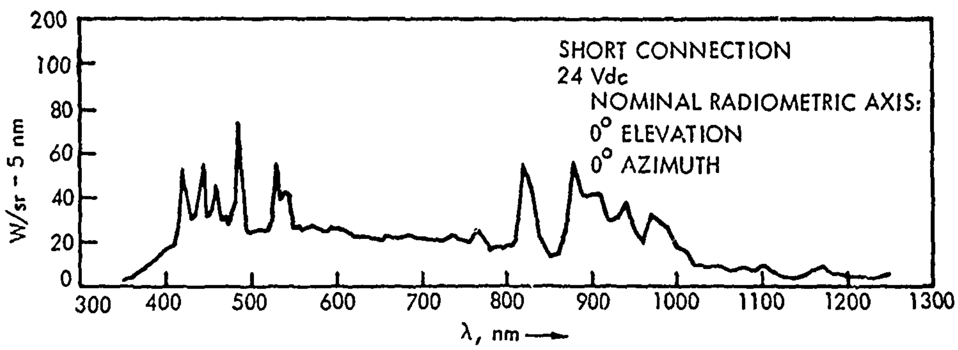

Figure 5-2. Spectral Peak Intensity of Whelen Strobe 7L

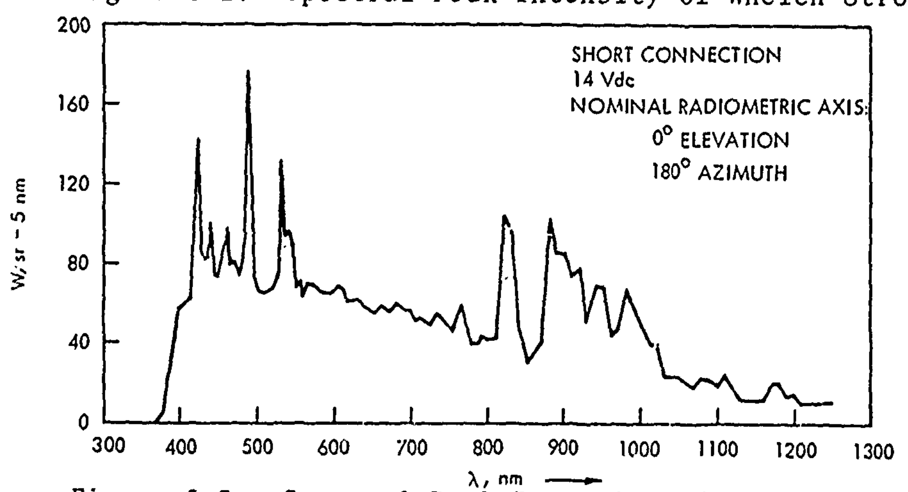

Figure 5-3. Spectral Peak Intensity of Grimes G-260 Strobe

1. The strobe being measured and the calibrated spectroradiometer were aligned at a fixed separation (either 100 or 300 cm) along the predefined radiometric axis.
2. The strobe and measurement equipment were allowed to warm up sufficiently, to ensure stable operation.
3. The spectroradiometer bandpass was stepped in 5 nm increments from 350 to 800 nm (center wavelength), wherein the half-intensity bandwidth (HIBW) was 5 nm, and again, the 10 nm increments from 700 to 1250 nm (center wavelength), wherein the HIBW was 10 nm. At each step peak pulse height was determined by visually averaging peak heights from a minimum of 10 pulses displayed on a storage screen, or by reading out pulse height from oscilloscope photographs in the case of Whelen Strobe #1.
4. The necessary computation to convert the spectroradiometer output to peak radiant intensity was performed.

The resultant measurements are tabulated in Table 5-1. Graphical representation of the data is in Figures 5-1, 5-2, and 5-3.

It is to be noted that the Whelen strobes were operated with the associated Whelen po ipplies at 24 VDC. This is acutally the worst case in an a' .e with a 24-volt system, wherein the alternator has a rated output of 28 volts. Typically, the voltage may be expected to be somewhat higher than 24 volts. Exactly what the typical operating voltage of the strobe power supply should be, has not been fully established. It has been determined, however, that the strobe output - for the strobes measured - is a function of the input voltage at the power supply. Strobe output is also a function of the length of cable between lamp and power supply.

An empirical study of voltage and cable length produced some results applicable to this section. Briefly, six Whelen strobes were operated at 24 and 28 volts into their power supplies, at each of four cable lengths. Strobe output was measured with the spectroradiometer at 800 nm with a 10 nm HIBW. The results shown in Figure 5-4 suggest how Table 5-1 and Figures 5-1 and 5-2

TABLE 5-1. SPECTRAL PEAK RADIANT INTENSITY W/SR - 5 NM

λ_{nm}	Whelen		Grimes	Hoskins	
	Lamp 1	Lamp 7		at 14 V	at 28 V
350	5.0	2.3	0.2	6.3	5.3
355	6.8	3.5	0.2	7.9	7.9
360	10.0	4.7	0.3	9.4	9.4
365	12.3	6.1	0.3	11.5	11.5
370	14.4	7.0	1.1	12.2	13.0
375	15.1	8.5	5.7	13.3	14.1
380	16.8	9.6	16.2	14.8	16.1
385	18.2	11.2	31.5	15.8	16.8
390	20.4	13.2	39.7	17.2	18.6
395	21.9	14.6	56.2	17.9	20.2
400	22.9	16.3	58.7	18.5	20.9
405	25.3	17.9	62.0	19.1	22.1
410	24.4	18.6	61.9	19.5	22.1
415	29.1	26.2	90.0	20.5	24.2
420	54.7	53.0	144.0	22.6	26.9
425	42.4	39.6	87.9	21.1	24.9
430	29.5	30.3	81.9	20.5	24.3
435	32.8	34.5	83.7	21.2	24.1
440	40.6	42.5	101.0	21.1	25.9
445	52.0	55.4	75.2	21.9	25.6
450	31.7	31.9	75.2	21.5	26.6
455	32.0	34.5	83.8	23.0	26.8
460	43.0	44.9	96.3	25.3	30.5
465	36.7	30.2	80.2	25.9	30.1
470	37.9	30.5	81.3	25.5	30.0
475	32.8	27.7	74.3	23.2	27.2
480	35.5	37.6	84.8	26.2	29.3
485	71.9	74.3	176.0	31.0	35.0
490	50.6	49.8	117.0	24.3	28.3
495	29.2	27.0	72.8	22.3	26.8
500	28.1	24.0	67.7	21.5	24.3
505	29.0	24.3	66.7	21.7	24.6
510	27.2	24.5	65.4	22.1	24.6
515	28.7	25.2	67.2	21.4	23.9
520	28.8	24.6	68.1	21.4	24.3
525	31.8	34.2	74.1	23.4	25.8
530	56.4	55.5	132 0	26.9	31.1
535	38.1	38.8	95.9	23.3	27.7
540	38.2	42.0	96.9	23.7	27.3
545	35.9	38.8	90.0	22.8	27.2

TABLE 5-1. SPECTRAL PEAK RADIANT INTENSITY W/SR - 5 NM (Continued)

λ_{nm}	Whelen		Grimes	Hoskins	
	Lamp 1	Lamp 7		at 14 V	at 28 V
550	28.0	26.3	68.3	21.2	24.3
555	29.9	26.8	71.4	20.3	23.4
560	27.4	25.9	64.7	21.9	25.0
565	28.9	26.4	70.3	21.7	24.8
570	28.6	27.1	70.5	20.9	24.4
575	27.0	27.4	68.9	20.3	24.2
580	27.4	25.7	66.5	20.4	23.9
585	25.7	25.4	65.9	19.9	22.8
590	26.8	25.0	65.9	19.4	23.0
595	27.5	26.5	65.9	20.1	23.6
600	27.8	25.6	66.8	19.3	24.0
605	26.5	26.1	68.6	20.6	23.8
610	27.1	25.4	67.2	19.8	23.6
615	24.0	23.7	62.0	19.2	23.1
620	25.5	23.1	61.6	18.9	22.4
625	24.6	22.2	62.1	19.4	22.4
630	24.8	23.0	61.7	18.0	22.3
635	25.2	22.9	61.0	18.7	21.7
640	22.8	22.3	59.5	18.2	21.2
645	29.5	21.6	58.4	18.7	22.2
650	30.0	21.3	57.4	18.3	21.3
655	29.9	21.1	57.0	17.3	21.2
660	29.3	22.2	58.4	17.9	20.9
665	28.9	21.5	57.1	18.7	21.4
670	29.5	21.8	57.9	18.2	20.8
675	29.9	22.2	57.3	18.3	21.4
680	30.9	22.9	60.1	19.3	21.5
685	29.8	23.4	59.0	19.0	21.6
690	28.1	22.6	57.0	18.2	20.8
695	27.7	22.1	57.6	17.6	20.2
700	29.4	22.0	56.0	16.8	19.9
705	26.6	21.0	52.6	17.2	19.0
710	26.8	21.1	53.2	17.8	20.0
715	26.8	21.6	53.1	17.0	19.7
720	23.8	20.1	50.8	16.9	18.5
725	24.9	20.3	50.8	17.1	18.9
730	27.3	22.1	54.2	18.2	20.0
735	27.7	23.1	55.2	17.7	20.0
740	26.6	21.5	52.8	16.9	19.1
745	24.3	20.7	50.3	16.5	18.8

TABLE 5-1. SPECTRAL PEAK RADIANT INTENSITY W/SR - 5 NM (Continued)

λnm	Whelen		Grimes	Hoskins	
	Lamp 1	Lamp 7		at 14 V	at 28 V
750	24.9	19.6	49.5	15.7	18.4
755	22.7	19.7	48.2	15.6	17.4
760	26.1	22.1	54.2	19.6	21.0
765	28.6	25.1	58.1	17.8	21.1
770	22.0	20.5	48.0	14.1	16.9
775	18.7	16.5	41.2	14.1	15.0
780	17.5	15.8	40.1	14.2	14.3
785	19.3	16.7	40.7	15.2	15.4
790	20.6	18.1	44.2	15.3	15.7
795	19.9	18.1	43.7	15.2	16.2
*800	20.3	17.0	42.5	15.5	15.9
810	24.7	20.1	43.4	16.9	16.3
820	63.8	55.7	103.8	40.1	42.0
830	50.9	44.7	96.6	40.6	44.7
840	23.6	21.1	51.8	19.4	24.4
850	14.4	12.9	31.1	10.9	12.8
860	16.7	14.4	32.3	11.7	12.2
870	27.1	25.5	43.0	17.3	15.8
880	64.5	56.5	98.9	47.7	44.3
890	45.5	41.7	88.5	37.1	38.2
900	46.7	40.7	87.1	34.4	34.4
910	45.7	41.8	75.3	33.8	33.8
920	32.2	29.7	79.5	28.1	31.9
930	30.5	30.5	52.5	22.7	22.3
940	40.6	37.3	70.1	33.6	33.6
950	28.7	27.7	69.4	25.6	27.2
960	21.7	19.6	45.4	17.7	17.7
970	35.7	32.0	48.8	23.9	22.7
980	31.3	28.6	66.9	25.8	25.8
990	32.2	27.3	59.7	26.3	26.8
1000	18.3	17.5	50.0	15.0	17.0
1010	17.9	15.4	40.6	15.1	15.9
1020	9.8	9.1	39.4	9.1	10.5
1030	9.3	8.6	24.3	7.7	8.2
1040	9.0	8.7	23.1	7.3	8.1
1050	9.4	8.5	23.9	7.8	8.2
1060	7.4	6.7	21.4	6.4	6.8
1070	8.1	7.7	18 9	6.1	6.2
1080	9.4	8.7	22.6	7.6	7.9
1090	7.3	6.3	23.1	7.1	7.8
1100	9.8	9.2	19.3	6.5	6.5

*Wavelength increments are 5 nm from 350 to 800 nm, and 10 nm from 800 to 1250 nm. Values tabulated are per 5 nm from 350 to 1250 nm. Therefore, when integrating from 800 to 1250 nm, tabulated [illegible] must be multiplied by 2.

TABLE 5-1. SPECTRAL PEAK RADIANT INTENSITY W/SR - 5 NM (Continued)

λ_{nm}	Whelen		Grimes	Hoskins	
	Lamp 1	Lamp 7		at 14 V	at 28 V
1100	9.8	9.2	19.3	6.5	6.5
1110	8.3	7.2	24.6	7.7	8.2
1120	4.8	4.3	19.9	4.4	5.4
1130	3.9	3.4	13.1	3.1	3.3
1140	4.1	3.4	11.9	2.9	3.1
1150	5.2	4.3	12.0	3.2	3.4
1160	7.5	6.7	12.9	4.2	4.5
1170	9.9	8.3	18.6	6.6	6.6
1180	6.1	5.4	20.6	6.2	6.5
1190	4.4	4.1	14.7	3.5	4.4
1200	4.0	3.6	14.8	3.1	3.1
1210	4.2	4.1	11.3	3.1	3.1
1220	4.1	4.1	11.3	3.0	3.0
1230	5.2	3.5	10.1	2.8	2.8
1240	5.9	3.2	10.3	2.7	2.2
1250	9.7	5.1	11.6	2.5	2.5

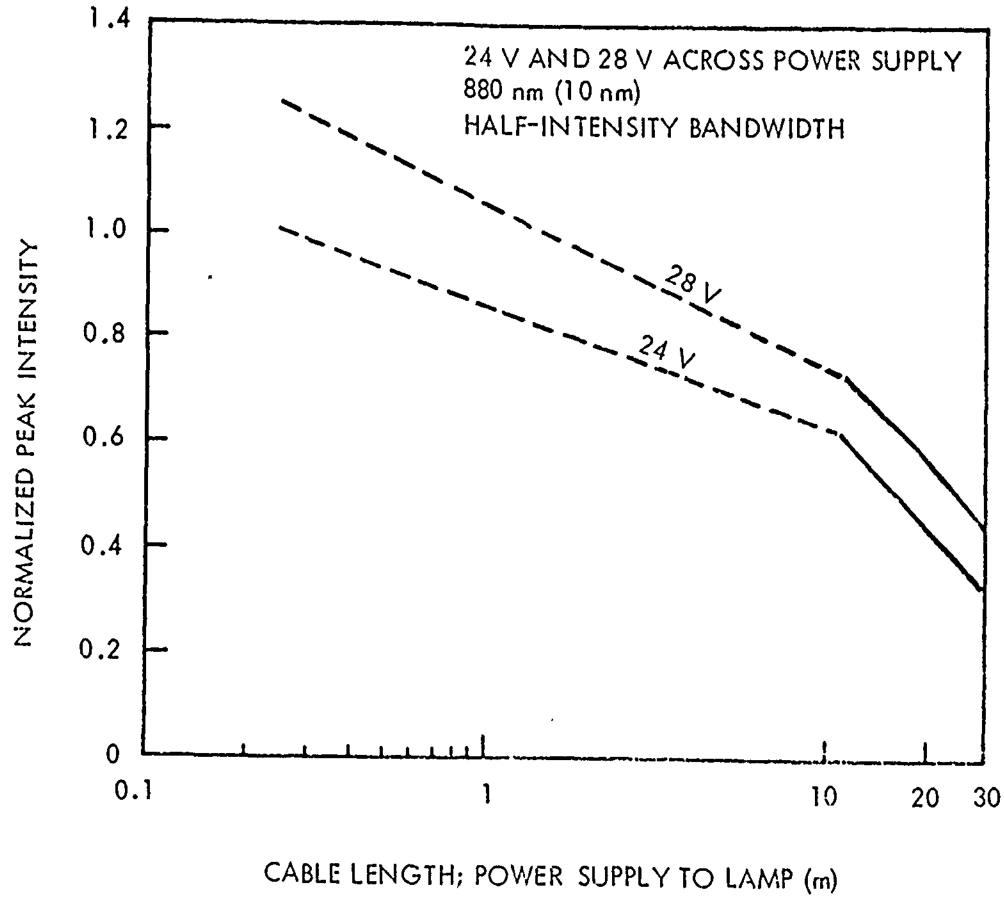

Figure 5-4. Normalized Peak Strobe Intensity Vs. Cable Length - Graphic Diagram

might be appropriately scaled, although this has not been proven outside the 880-nm region.

The outputs of several strobes were compared on a relative basis for two different broadband detection modes. In one mode, the detector was a silicon photodiode with no optical filtering, while in the other mode an RG-780 filter was used. Six Whelen strobes were operated consecutively from a single power supply at each of two voltages. The Grimes strobe lamps were all operated at 14 volts. To allow comparison, one red-filtered Grimes strobe was included as well. The detector was positioned on the 0° elevation, 0° azimuth axis in all cases. Table 5-2 lists the normalized broadband peak irradiance data, allowing the following interpretations:

TABLE 5-2. NORMALIZED BROADBAND PEAK IRRADIANCE OF STROBES

Strobe*	Detector without Filtering Strobe @14V	24V	28V	Detector with RG-780 Filter Strobe @14V	24V	28V
Whelen		.38	.54		.16	.22
Whelen 1L		.38	.55		.17	.21
Whelen 2		.45	.59		.17	.24
Whelen 3L		.45	.60		.19	.24
Whelen 7L		.40	.54		.15	.19
Whelen 8		.41	.60		.17	.24
Grimes G-260	1.00			.39		
Grimes G-294	1.00			.38		
Grimes G-119 (red)	.66			.39		

Strobe	Detector without Filtering Strobe @14V	28V	Detector with RG-780 Filter Strobe @14V	28V
SS-1	.30	.32	.13	.14
G-260	1.00		.39	

*Whelen power supply #1 was used with all Whelen strobe lamps. All strobe lamps were operated with short connections to the power supply.

1. With all strobes, the radiant power detected through the RG-780 filter is about 40 percent of that detected without the filter.
2. With the Whelen strobes, an increase in power supply voltage produces proportionally more output in the visible region than in the near-IR spectral region.
3. There is little change in the relative spectral distribution in the output of strobe SS-1, as the input voltage changes from 14 to 28 VDC.

Keeping in mind that the data in Table 5-1 must be scaled for different voltages and/or cable lengths, the following Table 5-3 presents a listing of integrated broadband peak radiant intensity derived from Table 5-1.

TABLE 5-3. INTEGRATED PEAK INTENSITY OF STROBES

Strobe	Integrated Peak Radiant Intensity	
	350 - 1250 nm	750 - 1250 nm
Whelen Strobe (.24 m cable 24V 0° EL., & 0° AZ.)	4282 W/SR	1985 W/SR
Whelen Strobe 7L (.16 m cable 24V 0° EL., 40° AZ.)	3903 W/SR	1817 W/SR
Grimes Strobe G-260 (.12 m cable 14V 0° EL., 180° AZ.)	9204 W/SR	3970 W/ST
Symbolic Displays Silver Star 1 14V (0° EL., 0° AZ.)	3080 W/SR	1515 W/SR
Symbolic Displays Silver Star 1 28V (0° EL., 0° AZ.)	3373 W/SR	1570 W/SR

To be noted in Table 5-3 is the relative amount of power above 750 nm. Approximately 45 percent of the power in the 350 - 1250 nm range is above 750 nm. A silicon photodiode filtered with a Schott RG 780-type filter would operate in this range. Note, too, that an RG 780 uncoated filter transmits approximately 90 percent at best, according to measurements made at NUSC/NL on a 2-nm thick sample. The effect of this filter is discussed from the viewpoint of electronic bandwidth considerations in Section 5.5 dealing with spectral analysis from 0 - 200 kHz.

5.3 SPECTRAL RADIANT ENERGY

To supplement the previous section, and to provide data of possible application in future PWI designs, the spectral distribution of energy in the output of Whelen strobe lamp #1 was measured in the following manner:

1. Whelen strobe #1 and the calibrated spectroradiometer were aligned at 100-cm separation along the 0° elevation, 0° azimuth radiometric axis.
2. The strobe and measurement equipment were allowed to warm up sufficiently to ensure stable operation.
3. The spectroradiometer bandpass was stepped in 5-nm increments from 350 to 800 nm (center wavelength), with a 5 nm HIBW, and again in 10 nm increments from 700 to 1250 nm (center wavelength), with a 10 nm HIBW. At each step, the pulse waveform displayed on an oscilloscope was photographed.
4. Narrow-band energy per pulse was obtained by measuring the area under each photographically-reproduced pulse shape via planimeter. The area under each curve was converted to energy via the appropriate scaling and calibration factors.

The resultant, reduced data are presented in Figure 5-5 and in Table 5-4.

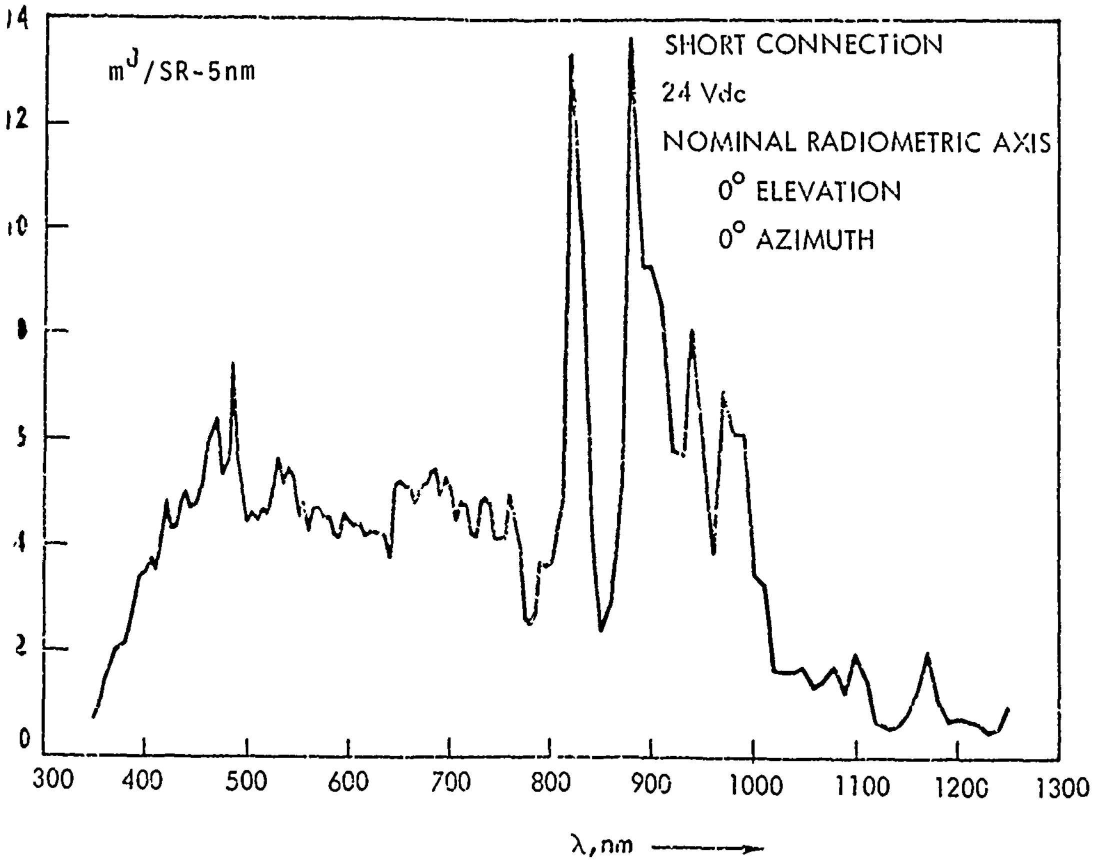

Figure 5-5. Spectral Radiant Energy of Whelen Strobe #1 Emitted per Steradian - Graphic Diagram

TABLE 5-4. SPECTRAL RADIANT ENERGY PER STERADIAN OF WHELEN STROBE 1

λ, nm	Joules x 10^{-3}/SR-5 nm	λ, nm	Joules x 10^{-3}/SR-5 nm	λ, nm	Joules x 10^{-3}/SR-5 nm
350	0.72	460	5.91	570	4.72
355	0.98	465	6.15	575	4.54
360	1.40	470	6.41	580	4.56
365	1.56	475	5.31	585	4.23
370	2 01	480	5.57	590	4.13
375	2.06	485	7.45	594	4.62
380	2.18	490	5.62	600	4.49
385	2.69	495	4.90	605	4.39
390	3.00	500	4.43	610	4.43
395	3.42	505	4.63	615	4.21
400	3.51	510	4.49	620	4.26
405	3.76	515	4.68	625	4.24
410	3.57	520	4.63	630	4.20
415	4.22	525	5.02	635	4.14
420	4.77	530	5.64	640	3.81
425	4.33	535	5.19	645	5.13
430	4.37	540	5.43	650	5.23
435	4.85	545	5.26	655	5.14
440	5.01	550	4.53	660	5.12
445	4.69	555	4.82	665	4.83
450	4.82	560	4.34	670	5.07
455	5.16	565	4.68	675	5.16

TABLE 5-4. SPECTRAL RADIANT ENERGY PER STERADIAN OR WHELEN STROBE 1 (Continued)

λ, nm	Joules x 10^{-3}/SR-5 nm	λ, nm	Joules x 10^{-3}/SR-5 nm	λ, nm	Joules x 10^{-3}/SR-5 nm
680	5.36	790	3.69	1000	3.51
685	5.43	795	3.66	1010	3.29
690	4.99	800	3.71	1020	1.67
695	5.30	810	4.75	1030	1.66
700	5.09	820	13.42	1040	1.66
705	4.50	830	10.04	1050	1.75
710	4.82	840	4.18	1060	1.36
715	4.76	850	2.40	1070	1.50
720	4.29	860	2.99	1080	1.74
725	4.21	870	5.08	1090	1.25
730	4.80	880	13.68	1100	2.01
735	4.91	890	9.31	1110	1.54
740	4.77	900	9.34	1120	.72
745	4.15	910	8.58	1130	.62
750	4.20	920	5.85	1140	.67
755	4.16	930	5.77	1150	.87
760	4.98	940	8.13	1160	1.40
765	5.48	950	5.41	1170	2.03
770	3.94	960	3.89	1180	1.12
775	2.66	970	6.99	1190	.73
780	2.54	980	6.14	1200	.78
785	2.76	990	6.14	1210	.73

λ, nm	Joules x 10^{-3}/SR-5 nm
1220	.69
1230	.52
1240	.59
1250	.97

5.4 RISE TIME, DURATION, AND DECAY TIME VERSUS WAVELENGTH

Temporal pulse characteristics were measured spectrally, as well as broadband, in order to provide further information on the effects on electronic signal bandwidth, due to the optical filtering of a detector. Rise time (10% - 90% of peak), duration (50% - 50%), and decay time (90% - 10%) were measured on photographs of the pulse shape, as detected in narrow-band by the spectroradiometer. The set of photographs were obtained for Whelen strobe #1 and is the same set described in Section 5-3 above. Table 5-5 and Figures 5-6, 5-7, and 5-8 contain these data.

To obtain comparison values, rise time, duration, and decay time were broadband-measured for three strobes using a silicon photodiode both with and without an RG-780 filter. Three lamps were operated with short connections (0.12 and 0.24.m) to their power supplies and two with an 11.08-m cable inserted between lamp and supply. One of the strobes (Whelen strobe #1) was operated with 24 and 28 volts, respectively, at the power supply input. The data are presented in Table 5-6.

In the case of Whelen strobe 1, which has been studied more extensively than the others made available to NUSC/NL, the narrow-band (i.e., 5 or 10 nm) pulse shape is decidely different than the broadband pulse shape observed (i.e., with a silicon photodiode either with or without an RG-780 filter). Narrow-band, the pulses are either fast-rising and sharply peaked at some of the visible lines or, everywhere else, are slower rising, with a pronounced double peak. Broadband, the pulses rise to a single peak at the slower rate.

Caution is advised in attempting to use these data in transforming to the temporal frequency domain (for detector electronics considerations). As shown in Section 5.5, empirical frequency analysis produces different results than those obtained from theoretical arguments as found in the report by Carlson et al, Reference 1.

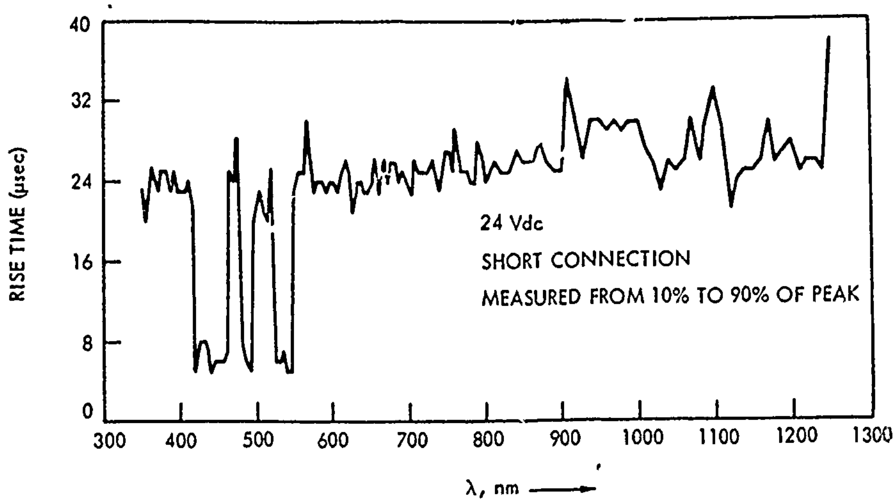

Figure 5-6. Rise Time of Whelen Strobe 1

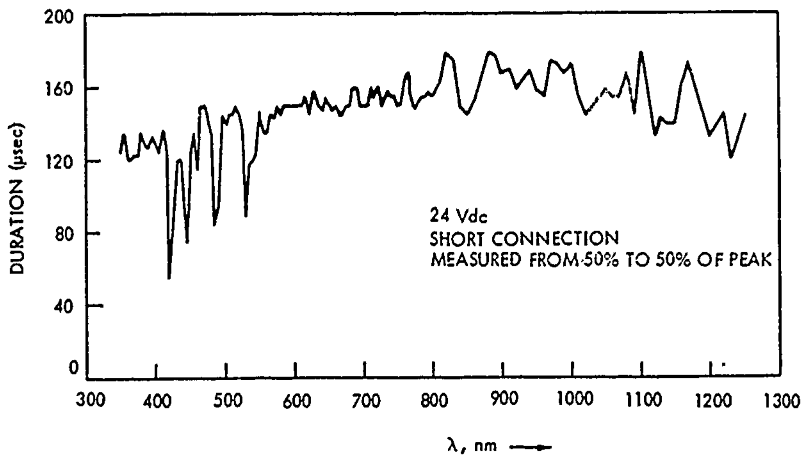

Figure 5-7. Duration of Whelen Strobe 1

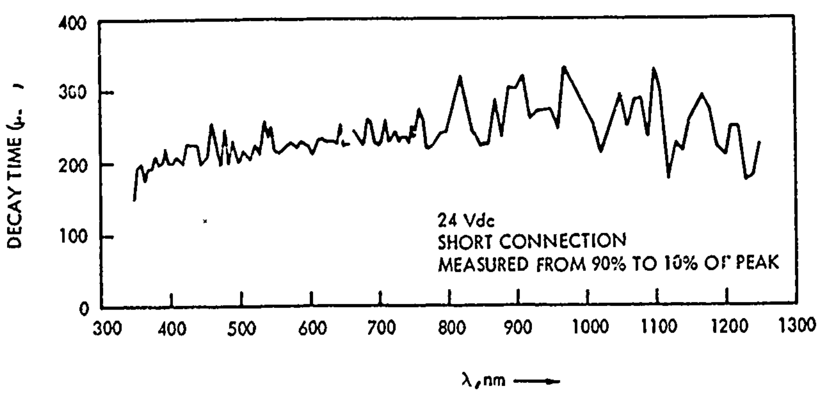

Figure 5-8. Decay Time of Whelen Strobe 1

TABLE 5-5. SPECTRAL RISE TIME, DURATION, AND DECAY TIME OF WHELEN STROBE 1 - SHORT CONNECTION, 24 VDC

λ, nm	10%-90% Rise Time μ sec	50%-50% Duration μ sec	90%-10% Decay Time μ sec	λ, nm	10%-90% Rise Time μ sec	50%-50% Duration μ sec	90%-10% Decay Time μ sec
350	23	125	155	450	6	128	208
355	20	135	195	455	6	135	210
360	23	120	200	460	7	115	255
365	25	120	175	465	25	150	228
370	23	123	193	470	24	150	205
375	25	123	193	475	28	140	200
380	25	135	210	480	8	135	245
385	23	128	198	485	6	85	200
390	24	128	200	490	5	95	230
395	23	133	220	495	20	145	210
400	23	128	200	500	22	140	203
405	23	125	200	505	23	145	215
410	24	137	205	510	21	145	210
415	21	124	200	515	20	150	205
420	5	55	200	520	25	145	215
425	8	95	225	525	6	135	225
430	8	120	223	530	6	90	215
435	7	120	223	535	7	118	260
440	5	100	225	540	5	120	235
445	6	75	198	545	5	123	250

TABLE 5-5. SPECTRAL RISE TIME, DURATION, AND DECAY TIME OF WHELEN STROBE 1 - SHORT CONNECTION, 24 VDC (Continued)

λ, nm	10%-90% Rise Time μ sec	50%-50% Duration μ sec	90%-10% Decay Time μ sec	λ, nm	10%-90% Rise Time μ sec	50%-50% Duration μ sec	90%-10% Decay Time μ sec
550	23	147	220	655	26	148	225
555	25	135	210	660	23	150	230
560	25	135	215	665	26	145	245
565	30	145	220	670	24	145	238
570	26	143	225	675	26	150	228
575	23	150	228	680	26	150	225
580	24	145	220	685	24	160	260
585	24	150	225	690	25	160	255
590	23	150	230	695	24	150	230
595	24	150	225	700	23	150	223
600	24	150	220	705	26	150	235
605	23	150	210	710	25	160	260
610	25	150	225	715	25	155	230
615	26	155	235	720	25	160	235
620	25	145	235	725	25	150	245
625	21	158	230	730	26	155	228
630	24	155	230	735	24	158	235
635	24	150	228	740	23	155	235
640	23	148	225	745	27	155	228
645	23	155	255	750	27	150	250
650	24	150	225	755	25	150	245

TABLE 5-5. SPECTRAL RISE TIME, DURATION, AND DECAY TIME OF WHELEN STROBE 1 - SHORT CONNECTION, 24 VDC (Continued)

λ, nm	10%-90% Rise Time μ sec	50%-50% Duration μ sec	90%-10% Decay Time μ sec	λ, nm	10%-90% Rise Time μ sec	50%-50% Duration μ sec	90%-10% Decay Time μ sec
760	29	165	275	920	30	160	260
765	25	168	260	930	26	165	270
770	25	155	220	940	30	170	273
775	25	148	220	950	30	160	275
780	24	153	225	960	29	155	245
785	24	155	230	970	30	175	330
790	28	155	240	980	29	173	313
795	27	158	243	990	30	168	295
800	24	155	250	1000	30	174	275
810	26	163	275	1010	27	155	255
820	25	180	320	1020	26	145	215
830	25	175	270	1030	23	150	235
840	27	150	240	1040	26	155	265
850	26	145	223	1050	25	159	295
860	26	153	225	1060	26	155	250
870	28	165	288	1070	30	155	285
880	26	180	235	1080	26	168	290
890	25	178	303	1090	30	145	235
900	25	168	303	1100	33	180	335
910	34	170	320	1110	29	158	295

TABLE 5-5. SPECTRAL RISE TIME, DURATION, AND DECAY TIME OF WHELEN STROBE 1 - SHORT CONNECTION, 24 VDC (Continued)

λ, nm	10%-90% Rise Time μ sec	50%-50% Duration μ sec	90%-10% Decay Time μ sec
1120	21	133	176
1130	24	143	228
1140	25	140	215
1150	25	140	260
1160	26	163	275
1170	30	174	296
1180	26	158	270
1190	27	145	220
1200	28	133	210
1210	25	140	250
1220	26	145	250
1230	26	120	175
1240	25	133	180
1250	38	145	225

TABLE 5-6. BROADBAND (OPTICAL) STROBE PULSE CHARACTERISTICS†

Strobe	Short Connection						Approx. 11.8-m Connection					
	No Filter			With RG-780 Filter			No Filter			With RG-780 Filter		
	RT*	DU**	DT***				RT	DU	DT	RT	DU	DT
Grimes G-260 14V	28	126	244	28	124	248	44	192	394	46	186	390
Whelen 1 24V	28	137	243	28	141	258	50	218	414	46	229	412
Whelen 1 28V	[illegible]	124	237	26	139	244	44	204	333	46	227	449
Symbolic Displays SS-1 14V	44	260	540	50	275	600						
Symbolic Displays SS-1 28V	42	250	560	50	270	600						

†Time in microseconds
*rise time (RT): 10% to 90% of peak
**duration (DU): 50% to 50% of peak
***decay time (DT): 90% to 10% of peak

5.5 SPECTRAL ANALYSIS FROM 0 TO 200 KILOHERTZ

A preliminary spectrum analysis of both the Grimes G-260 and Whelen 1 strobes was undertaken for several reasons. First, an examination of pulse shape spectrally and broadband, in the optical frequency domain, shows certain discrepancies that could lead to underestimating the power spectrum over 40 kHz. Second, using a silicon photodiode detector, the pulse shape observed with the "bare" detector was very much like that observed with a visible-blocking filter (RG-780) before the detector. Yet, on the basis of the spectral pulse shape data, a diminution of high-frequency (40 kHz) power would be expected in blocking radiation below 700 nm. Third, from a practical point of view, an empirical spectrum analysis is very nearly as easy to perform as a theoretical analysis and obviates the simplifying assumptions sometimes implicit in the theoretical approach.

Spectral analysis, then, was performed using an EG&G "lite-mike" detector in an unfiltered mode, as well as with an RG-780 filter. The output of the detector, with the typical silicon response, was fed into a Tektronix 564B storage oscilloscope with an SL5 spectrum analyzer plug-in. The displayed spectrum was subsequently photographed.

The spectrum analyzer was adjusted for two sweeps; 0 - 200 kHz with a center frequency of 100 kHz; and 0 - 10 kHz with a center frequency of 5 kHz. The strobe lamps were operated with short and long connections to their respective power supplies.

The Whelen strobe was operated at 24 VDC, as well as 28 VDC across its power supply. The spectrum analyzer photographs, along with the corresponding pulse shapes, are represented in Figures 5-9 through 5-14.

Figures 5-9 through 5-14 illustrate one point particularly well, and that is the effect of the RG-780 filter on the power spectrum. It is apparent that there is very little change in pulse shape, in going from an unfiltered silicon detector to an RG-780 filtered silicon detector. Yet, there is a significant effect on the pulse power spectrum between 20 kHz and 100 kHz, with the IR filter producing an effect equivalent to a low-pass, post-detection electronic filter.

Figure 5-9 is throughout consistent with the power theorem for transforms which in effect, is a statement of the conservation of energy from the time domain to the frequency domain. It can be seen in Figures 5-9(A) and 5-9(B) that the addition of the filter has the effect of scaling the pulse downward by about 55 percent. Looking at the power spectra in Figure 5-9(C), however, the filter has depressed the curve by only 25 percent (approximately). Thus, Figure 5-9(D) appears reasonable to the effect that a severe reduction in power, due to the IR filter, would take place somewhere above 10 kHz. This effect is noted for the short connection case with both the Grimes and Whelen strobes. With the 11.08-m cable between lamp and power supply - with either the Grimes or Whelen strobe - the high frequencies are suppressed to the extent that the IR filter produces a less significant frequency - specific effect on the power spectrum.

5.6 RADIATION GEOMETRY

Measurements in this section relate to the determination of strobe beam patterns. A sample of three strobes was used to supply independent verification of data previously obtained elsewhere. These strobes are described as "unidirectional-annular" in Section 3. Figures 5-15 through 5-18 illustrate the angle convention for describing the radiometric axis.

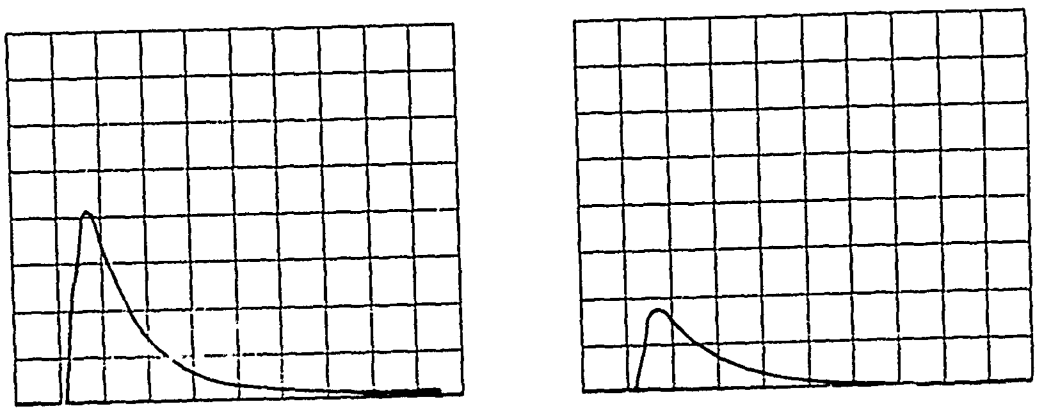

(A) NO FILTER

(B) WITH RG-780 FILTER

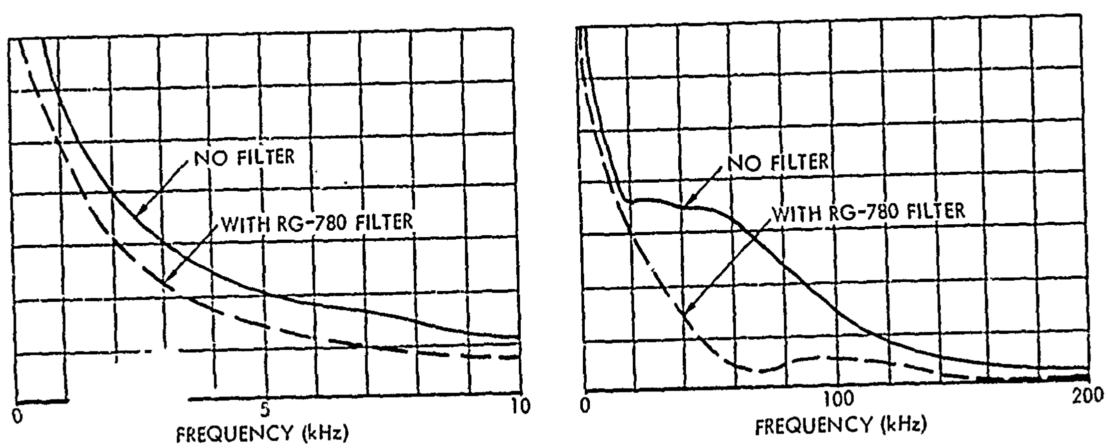

(C) POWER SPECTRA FOR (A) AND (B) ABOVE

(D) POWER SPECTRA FOR (A) AND (B) ABOVE

Figure 5-9. Pulse Shapes and Power Spectra for Grimes Strobe at 14 VDC, 0.12-m Connection; Scale 0.05 V/DIV. X 100, μSec/Div.

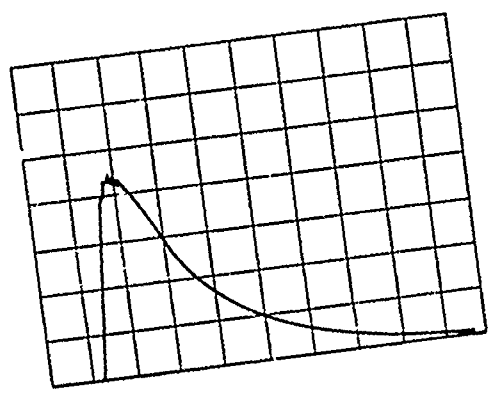

(A) NO FILTER

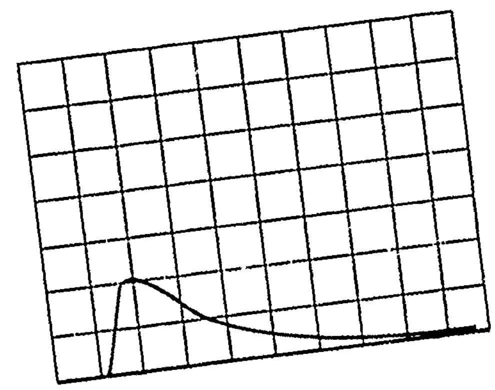

(B) WITH RG-780 FILTER

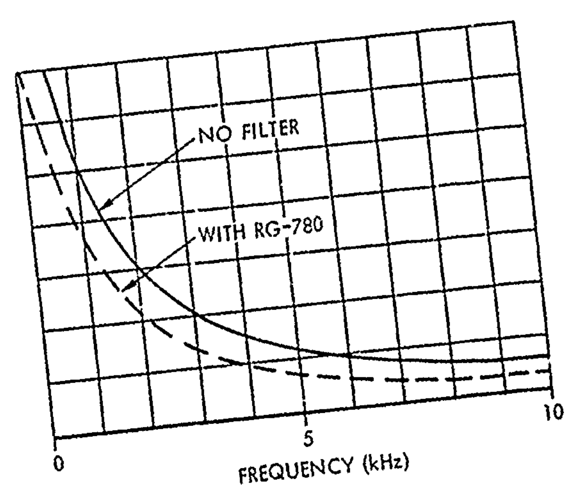

(C) POWER SPECTRA FOR (A) AND (B) ABOVE

Figure 5-10. Pulse Shapes and Power Spectra for Grimes Strobe G-260 at 14 VDC, 11.08-m Connection; Scale 0.02 V/DIV. X 100 μSec/Div.

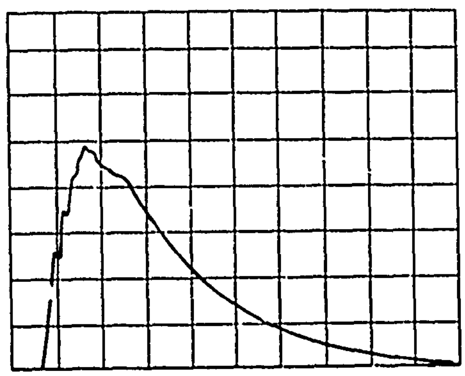

(A) NO FILTER

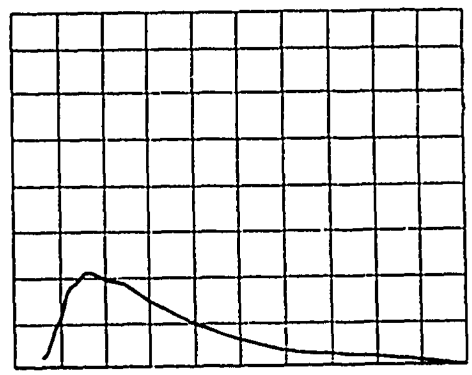

(B) WITH RG-780 FILTER

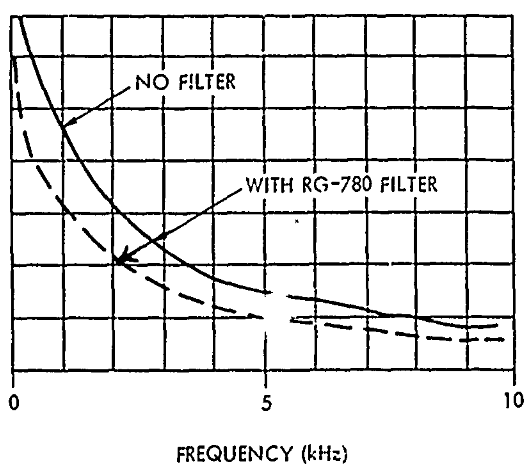

(C) POWER SPECTRA FOR (A) AND (B) ABOVE

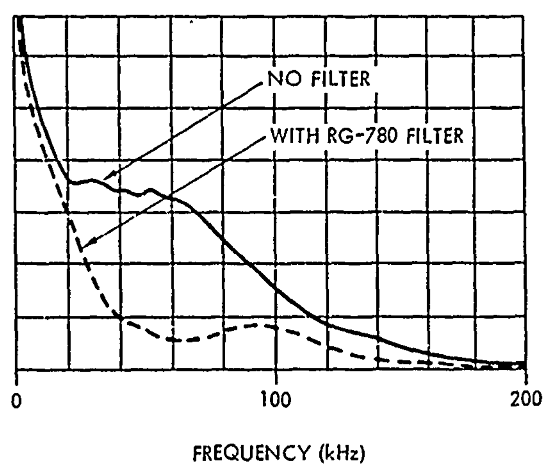

(D) POWER SPECTRA FOR (A) AND (B) ABOVE

Figure 5-11. Pulse Shapes and Power Spectra for Whelen Strobe #1 at 24 VDC, 0.24-m Connection; Scale 0.05 V/DIV. X 50 μSec/Div.

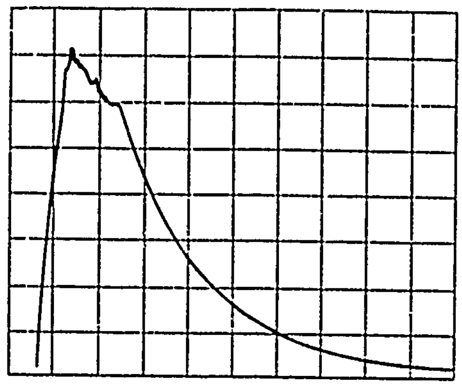

(A) NO FILTER

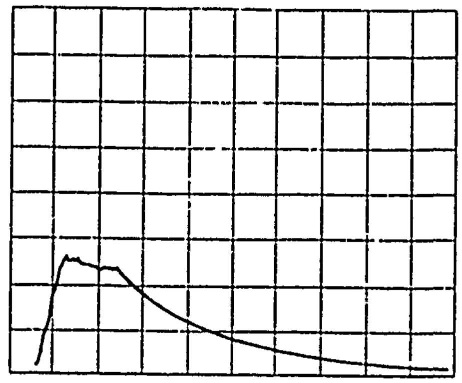

(B) WITH RG-780 FILTER

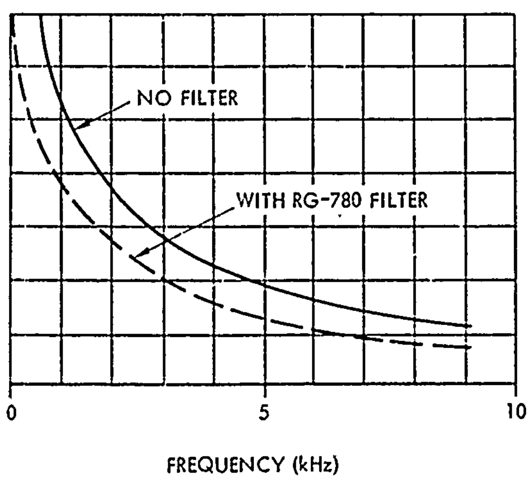

(C) POWER SPECTRA FOR (A) AND (B) ABOVE

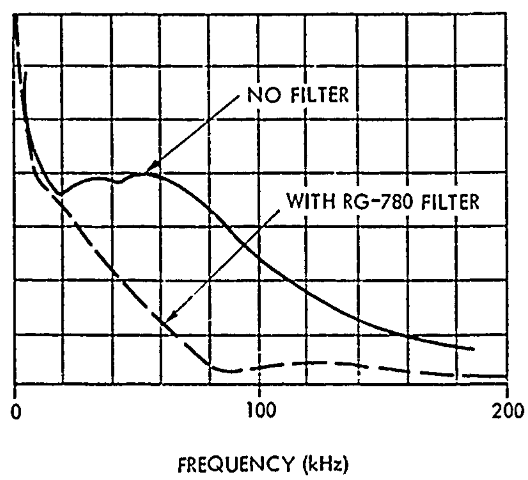

(D) POWER SPECTRA FOR (A) AND (B) ABOVE

Figure 5-12. Pulse Shapes and Power Spectra for Whelen Strobe #1 at 28 VDC, 0.24-m Connection; Scale 0.02 V/DIV. X 50 μSec/Div.

(A) NO FILTER

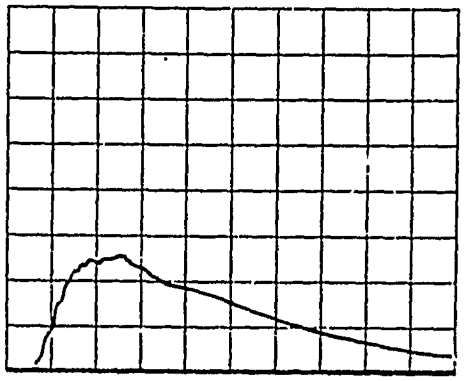

(B) WITH RG-780 FILTER

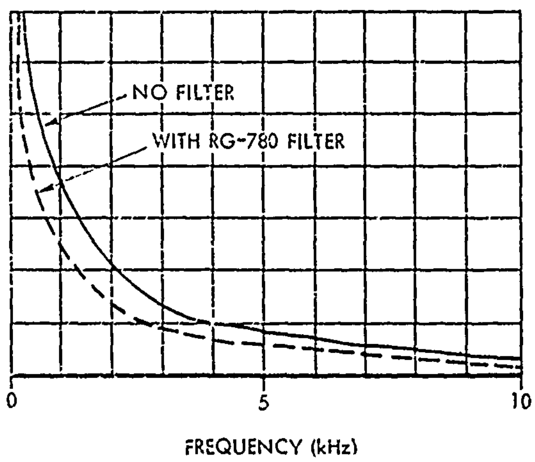

(C) POWER SPECTRA FOR (A) AND (B) ABOVE

Figure 5-13. Pulse Shapes and Power Spectra for Whelen Strobe #1 at 24 VDC, 11.08-m Connection; Scale 0.02 V/DIV. X 50 μSec/Div.

(A) NO FILTER
SCALE 0.5 V/DIV. X 50
μSEC/DIV.

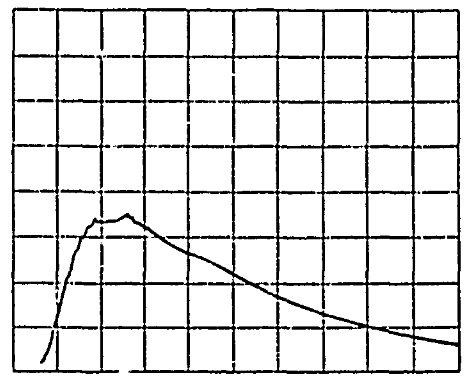

(B) WITH RG-780 FILTER
SCALE 0.02 V/DIV. X 50
μSEC/DIV.

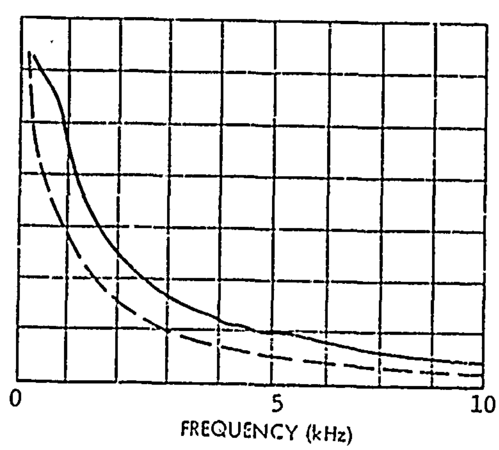

(C) POWER SPECTRA FOR (A) AND (B) ABOVE

Figure 5-14. Pulse Shape and Power Spectra for Whelen Strobe #1 at 28 VDC; 11.08-m Connection

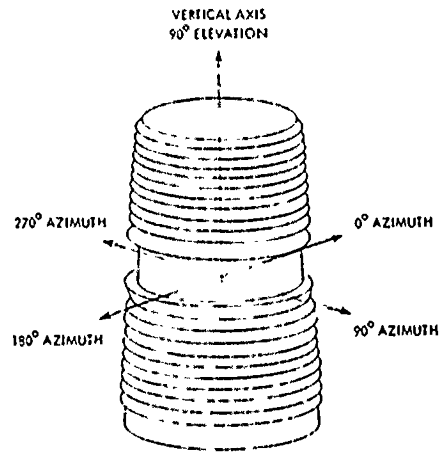

Figure 5-15. Whelen Strobe Lamp

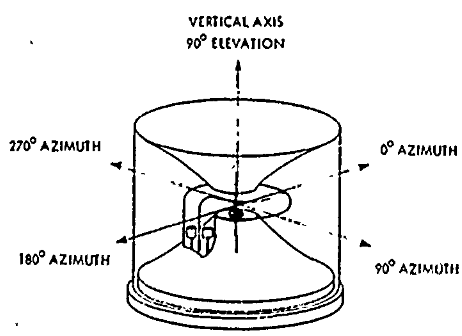

Figure 5-16. Grimes Strobe Lamp

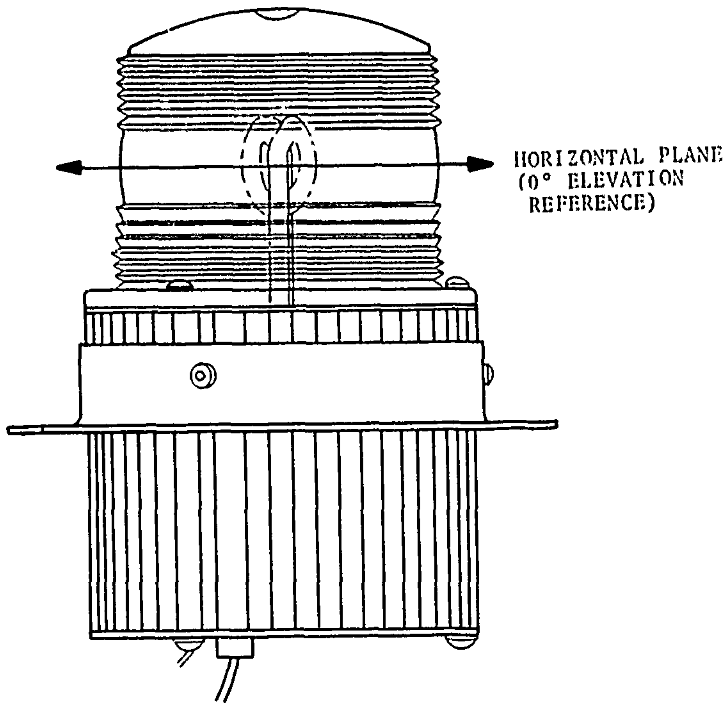

Figure 5-17. Side View of the SS-1 Strobe Lamp

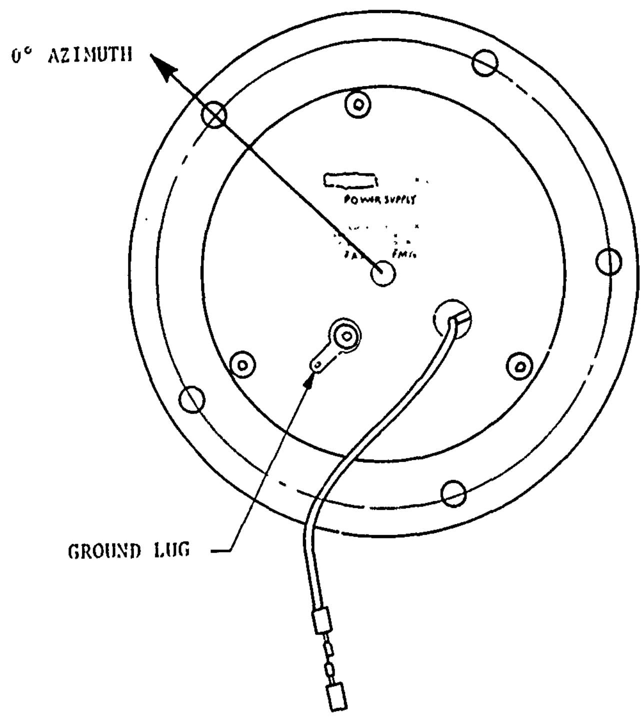

Figure 5-18. Bottom View of the SS-1 Strobe Lamp

The horizontal plane (i.e., 0° elevation) is parallel to the base in both cases. For the Whelen strobe (two of the same type were used), the 0° azimuth axis was established by noting marks on the base left by previous researchers at MIT. Nominally, the flash-tube anode is supposed to face an observer looking at the lamp along the 0° azimuth, 0° elevation axis. This is only approximately the case with the Whelen strobes on hand at NUSC/NL. This observation is made only to caution against assumptions regarding anode position and the 0° elevation, 0° aximuth, 0° axis. (The data is plotted in Figures 5-14 to 5-23.)

The Grimes strobe was defined to have a 0° azimuth, 0° elevation axis opposite the lamp electrodes (see Figure 5-24). This is contrary to the MIT convention.

The angular distribution of peak irradiance was measured in the following manner:

1. The lamp being measured was mounted in a special yoke and cradle assembly which was, in turn, mounted on a rotary table.

2. The modified spectroradiometer was employed as the detector, mounted at 300 cm from the lamp.

3. Initial alignment included centering of the lamp on the rotary table axis and leveling the lathe bed, to assure verticallity of the rotary table axis. The detector was mounted at the same height as the lamp. Final alignment included the use of an autocollimator, to check the zeroing of both axes about which the lamp was to rotate.

4. The spectroradiometer was adjusted to pass a narrow band of radiation, and the measurements then proceeded. Two types of scanning were employed. One type of scan (azimuthal) was about the vertical axis (360° azimuth scan at 0° elevation) in 5° steps. The other type of scan (elevational) was about a horizontal axis (a 360° elevational scan about a preset horizontal axis in graded increments). These increments were 5° from -30° to +30° relative to the horizontal plane and 15° elsewhere.

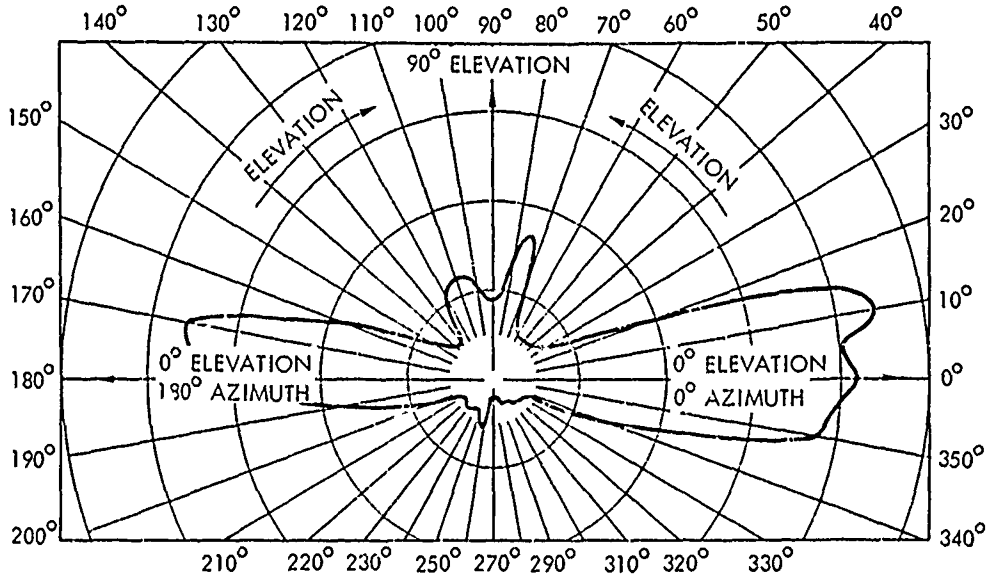

A. ELEVATIONAL SCAN THROUGH 0° AZIMUTH

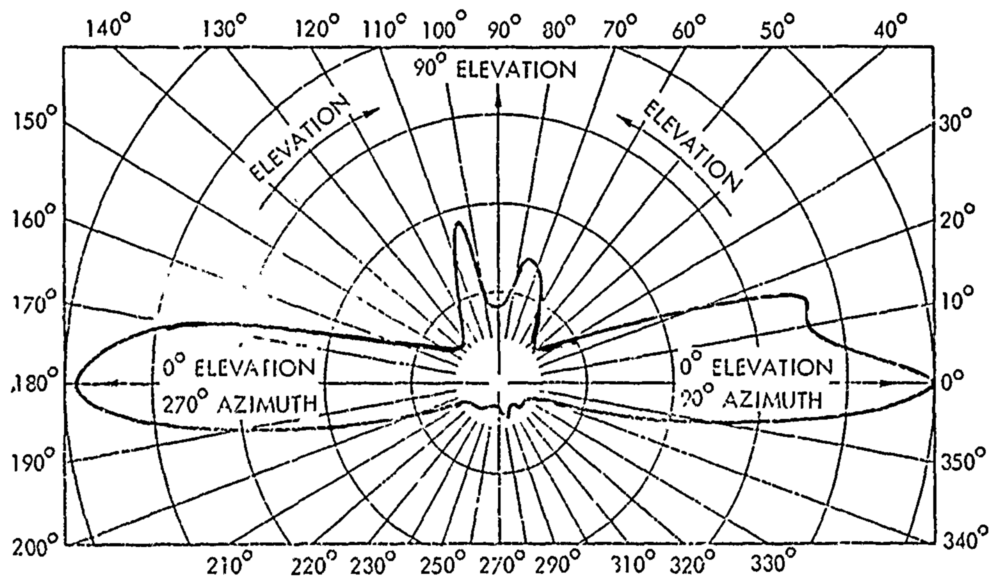

B. ELEVATIONAL SCAN THROUGH 90° AZIMUTH

Figure 5-19. Angular Distribution of Radiance at 485 nm (5-nm HIBW) for Whelen Strobe #1

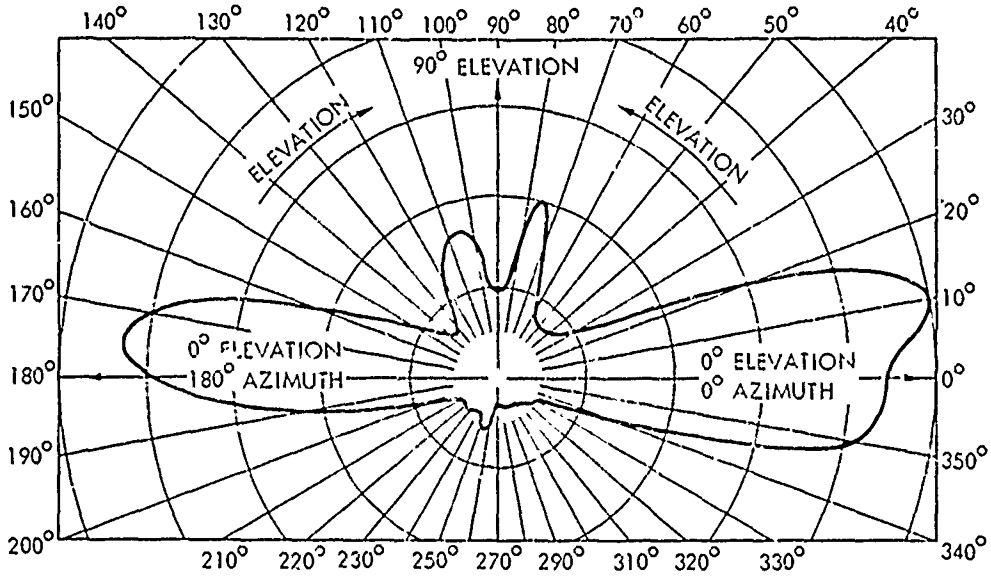

A. ELEVATIONAL SCAN THROUGH 0° AZIMUTH

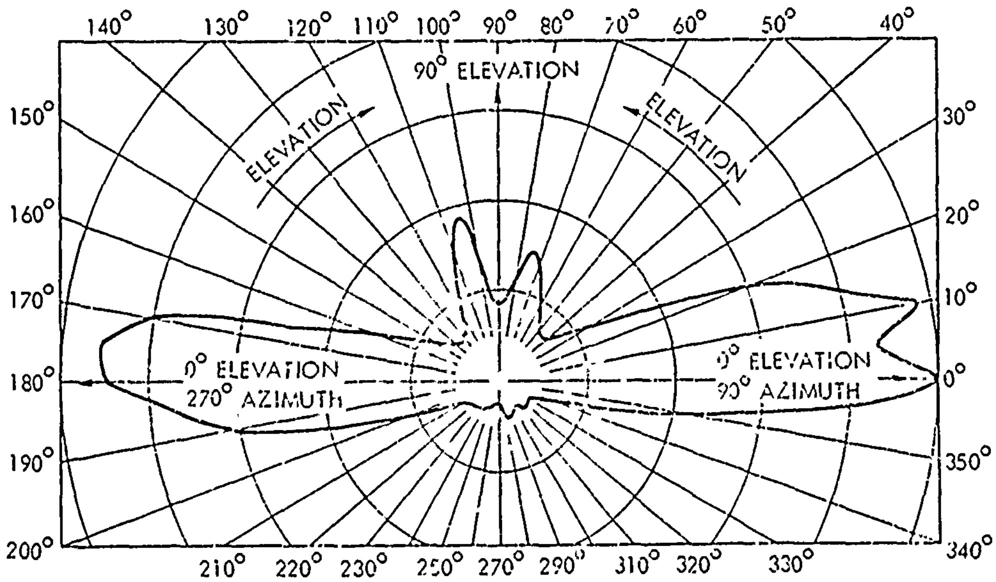

B. EVELATIONAL SCAN THROUGH 90° AZIMUTH

Figure 5-20. Angular Distribution of Radiance at 650 nm (5-nm HIBW) for Whelen Strobe #1

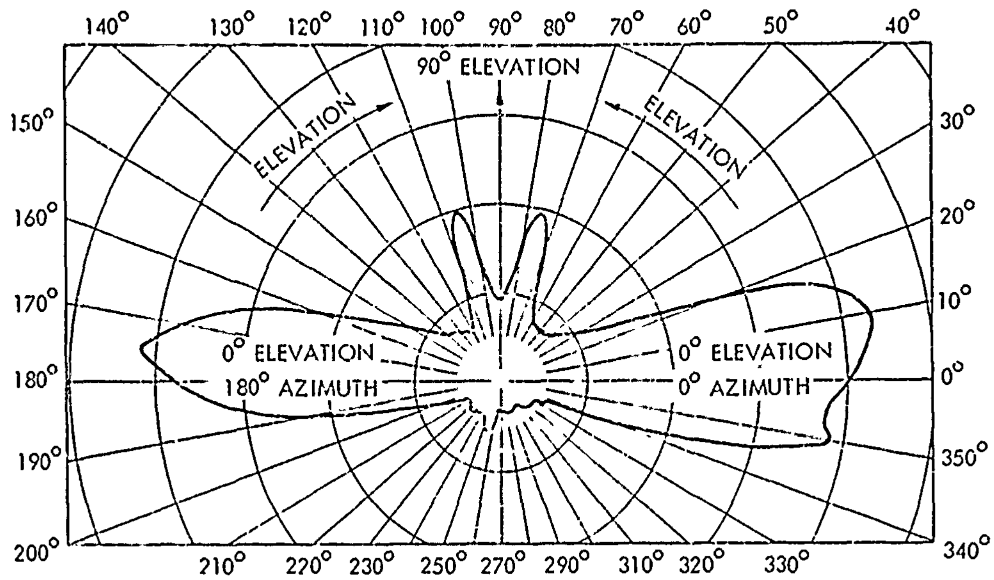

A. ELEVATIONAL SCAN THROUGH 0° AZIMUTH

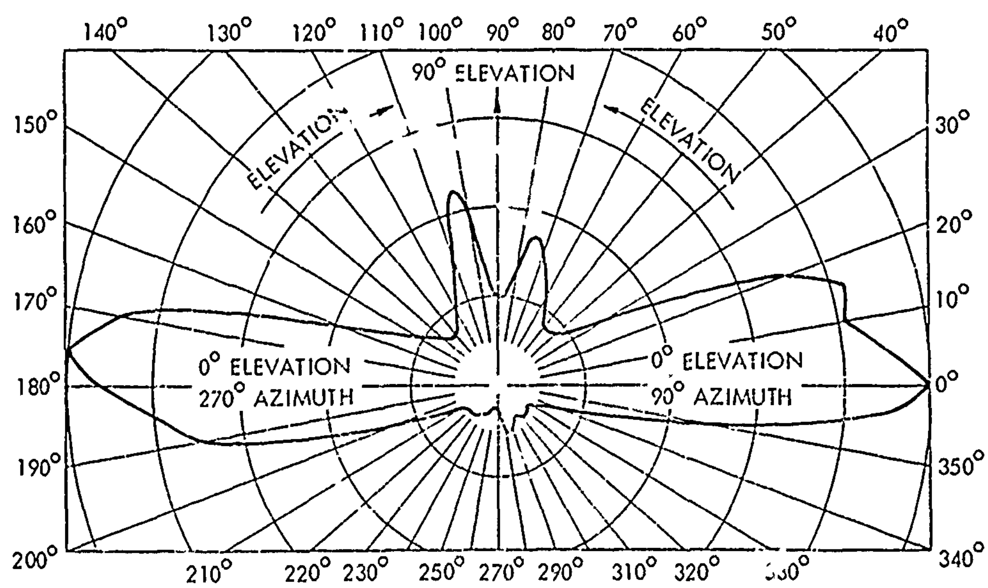

B. ELEVATIONAL SCAN THROUGH 90° AZIMUTH

Figure 5-21. Angular Distribution of Radiance at 880 nm (5-nm HIBW) for Whelen Strobe #1

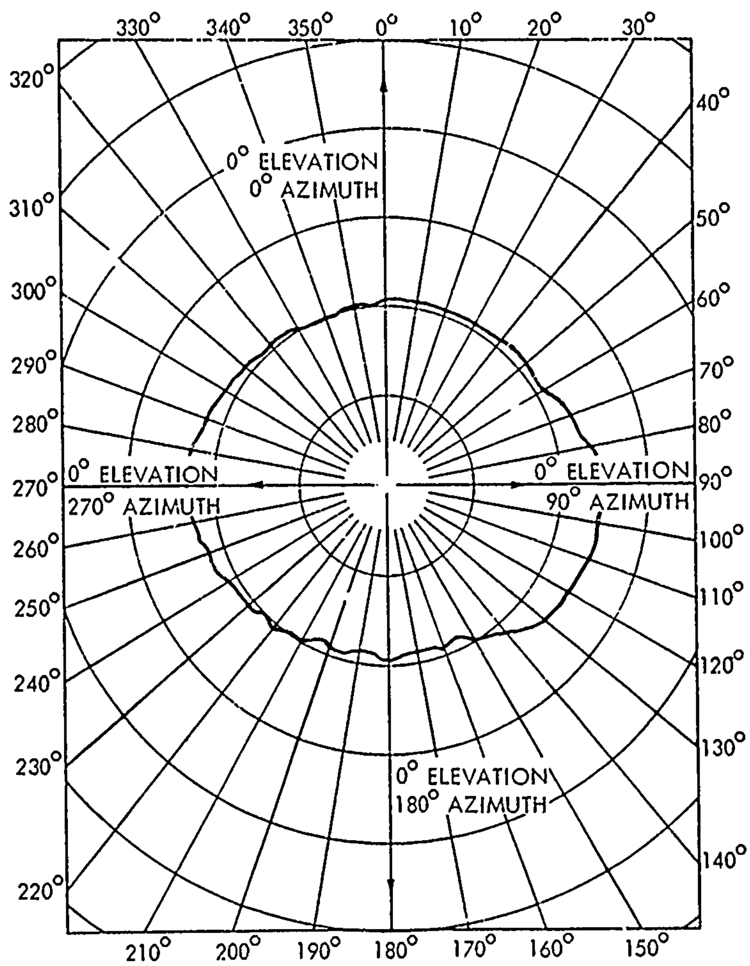

C. AZIMUTHAL SCAN AT 0° ELEVATION

Figure 5-21. Angular Distribution of Radiance at 880 nm (5-nm HIBW) for Whelen Strobe #1 - Continued

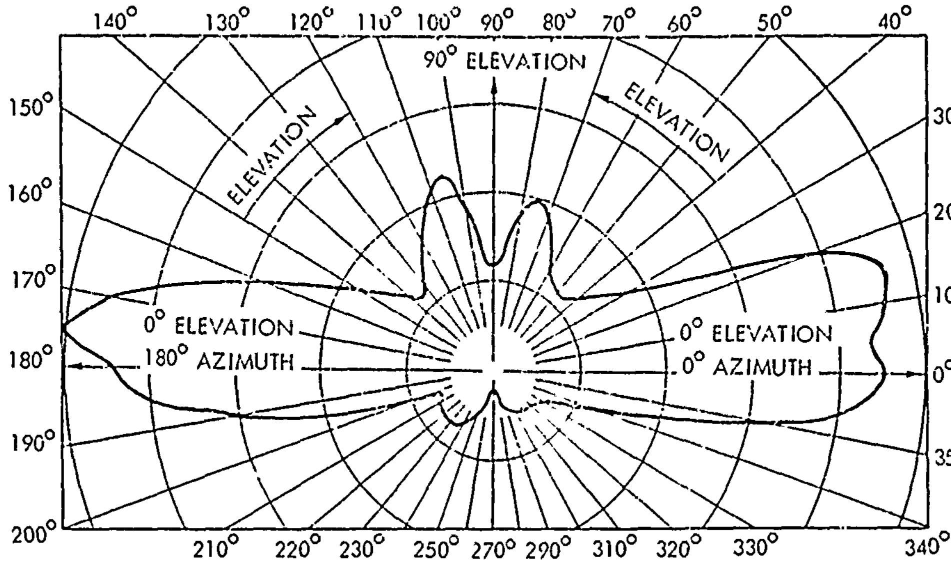

A. ELEVATIONAL SCAN THROUGH 0° AZIMUTH

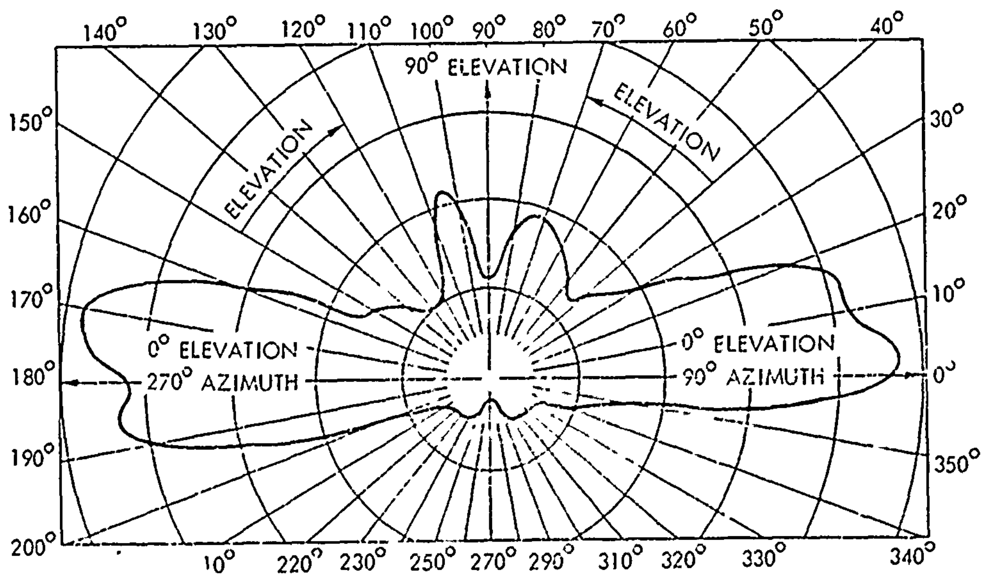

B. ELEVATIONAL SCAN THROUGH 90° AZIMUTH

Figure 5-22. Angular Distribution of Radiance at 880 nm (5-nm HBW) for Whelen Strobe #7L

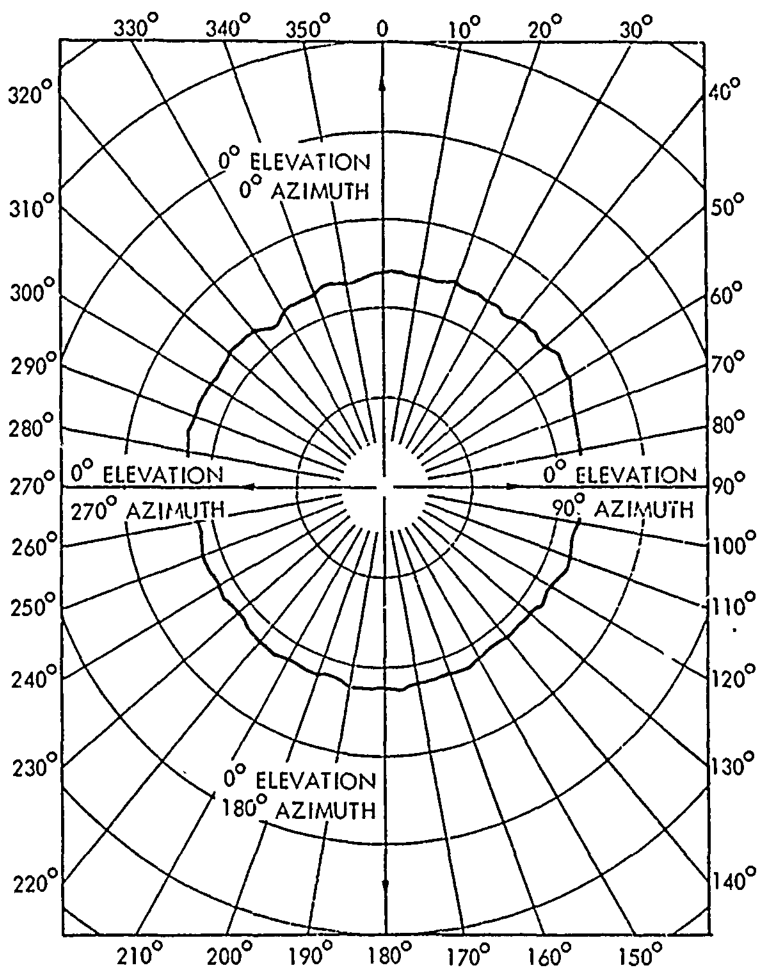

C. AZIMUTHAL SCAN AT 0° ELEVATION

Figure 5-22. Angular Distribution of Radiance at 880 nm (5-nm HIBW) for Whelen Strobe #7L (Continued)

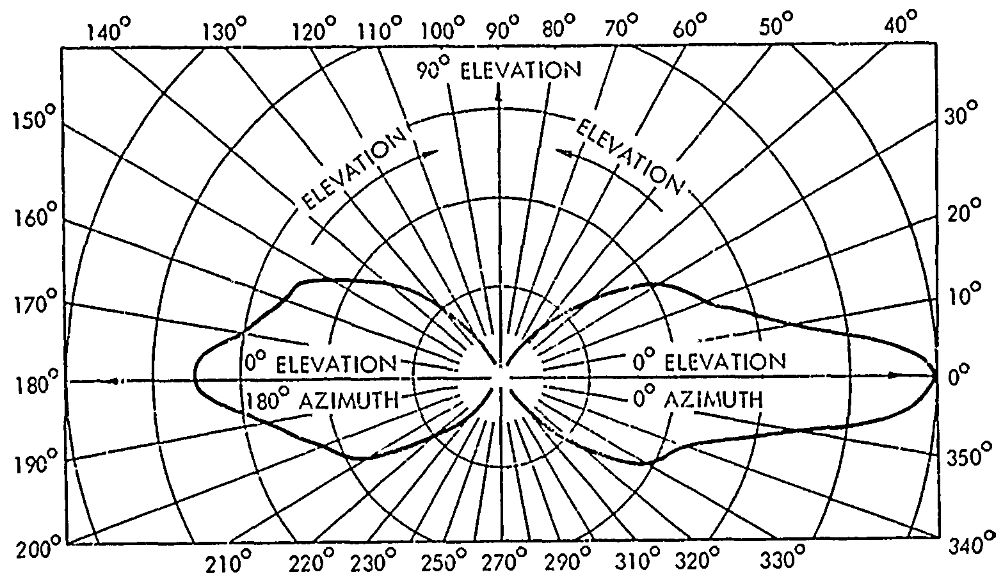

A. ELEVATIONAL SCAN THROUGH 0° AZIMUTH

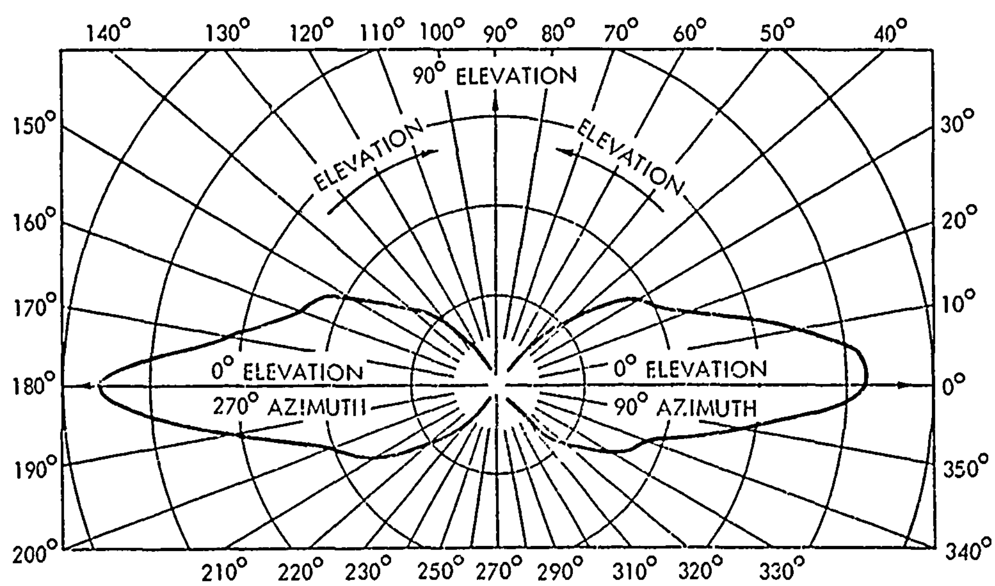

B. ELEVATIONAL SCAN THROUGH 90° AZIMUTH

Figure 5-23. Angular Distribution of Radiance at 880 nm (5-nm HIBW) for the Grimes G-260 Strobe

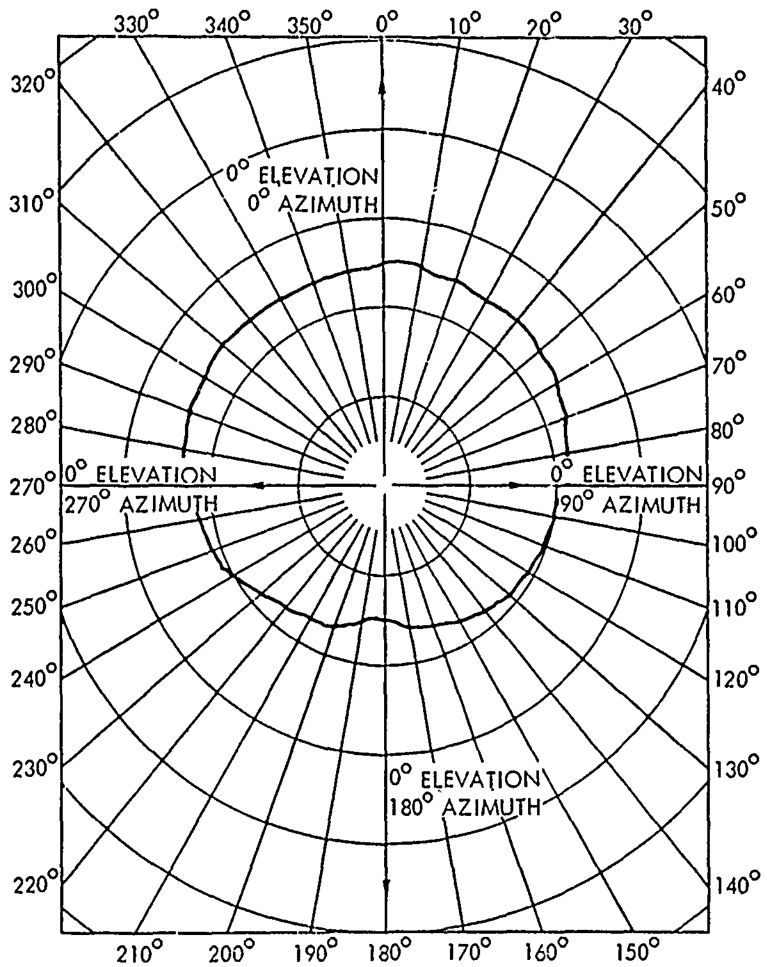

C. AZIMUTHAL SCAN AT 0° ELEVATION

Figure 5-23. Angular Distribution of Radiance at 880 nm (5-nm HIBW) for the Grimes G-260 Strobe - Continued

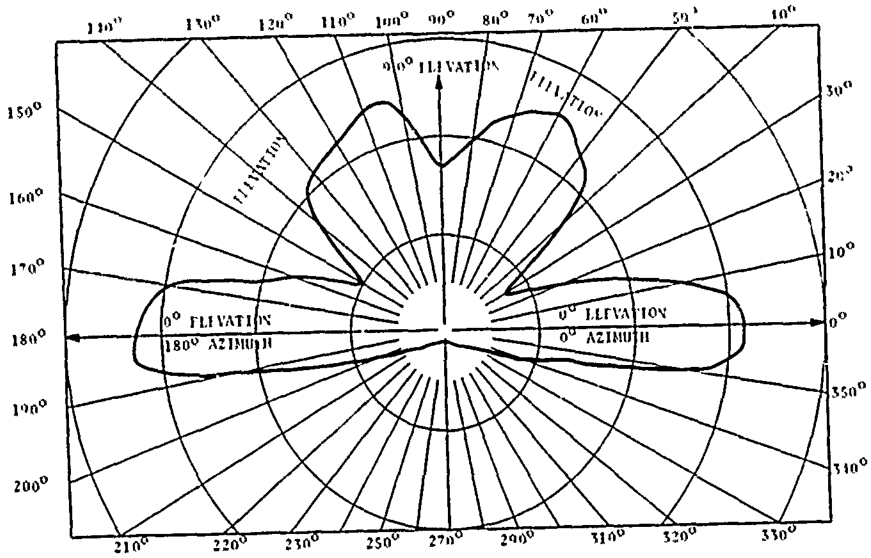

A. ELEVATIONAL SCAN THROUGH 0° AZIMUTH

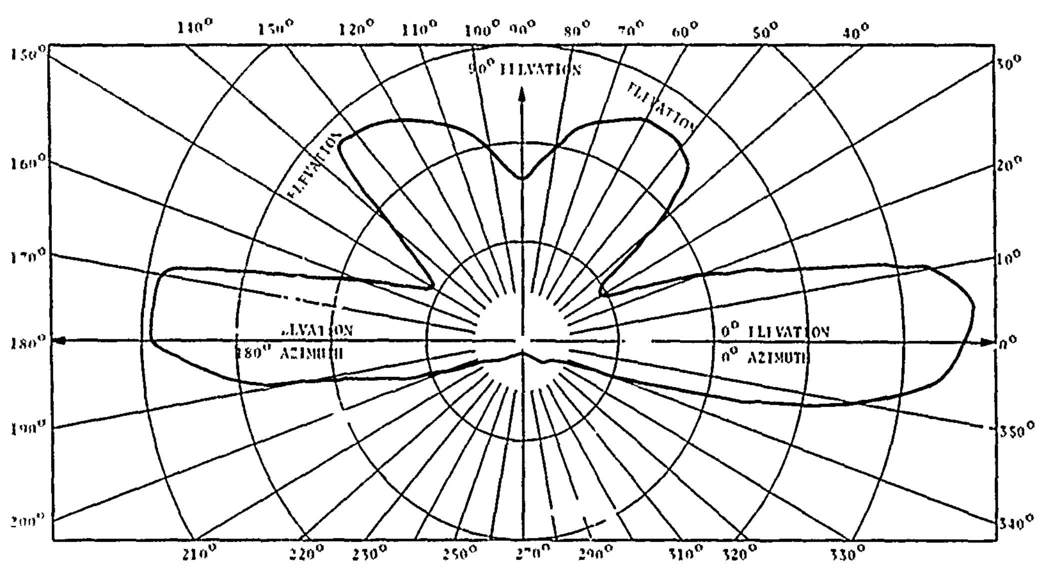

B. ELEVATIONAL SCAN THROUGH 90° AZIMUTH

Figure 5-24. Angular Distribution of Radiance at 880 nm (5-nm HIBW) for the SS-1 Strobe

Measured values of peak irradiance were tabulated, normalized at the highest value, and plotted. Elevational scans were done in pairs with the scan axes being separated by 90 degrees in the horizontal plane. In this case, normalization was to the highest value in the pair of scans.

Most of the scans were made with a 10-nm bandpass at 880-nm. In the case of Whelen strobe #1, elevational scan pairs were obtained at 485 nm (5-nm HIBW) and 650 nm (5-nm HIBW) as well. The data are plotted in Figures 5-19 through 5-23.

Referring to Figures 5-19 through 5-24, the following observations are made:

1. Elevational variations in beam pattern as a function of wavelength are no greater than variations at a single wavelength from lamp to lamp.
2. The Whelen strobes consistently radiate more strongly above the horizontal plane than below.
3. The beam profile of the Symbolic Displays SS-1 in the horizontal plane is ragged.

5.7 PHOTOMETRIC CALCULATIONS

Utilizing the absolute spectral peak radiant intensity data from Table 5-3, the peak luminous intensity was calculated. The calculations involved piecewise multiplication of the spectral peak radiant intensity data with the photopic luminosity curve, numerical integration of the series of products, and finally converting the total to peak lumens per steradian, i.e., peak candle power expressed in candles.

The calculated photometric data are listed in Table 5-7. Included also is the quantity of light for Whelen #1 strobe in lumen (seconds per steradian), i.e., beam candle power seconds (BCPS), on the 0° elevation, 0° azimuth axis.

TABLE 5-7. PHOTOMETRIC PROPERTIES OF STROBES

Strobe	Peak Luminous Intensity In Candles (CD)	Quantity of Light In Beam Candle Power Seconds (BCPS)
Whelen 1 (24V)	4.60×10^5	69.4
Whelen 7L (24V)	4.42×10^5	----
Grimes G-260 (14V)	1.10×10^6	----
Symbolic Displays SS-1 (14V)	3.14×10^5	----

5.8 STROBE STABILITY

To assess the stability of peak power from pulse-to-pulse for a given strobe, a series of pulse height observations was made for each of several conditions. Using a silicon photodiode detector, 200 pulse heights were observed for Whelen strobe #1 both with a 0.24-m connection to its power supply and with an 11.08-m cable between lamp and supply.

With the Grimes G-260 strobe (0.12-m connection to its power supply), 200 pulses were observed with the unfiltered silicon detector, and 120 pulses were observed with the detector filtered with an RG-780 filter. The standard deviation from the arithmetic mean was determined for each of the four distributions of peak power and is listed in Table 5-8.

To assess the stability of peak power from pulse-to-pulse for strobe SS-1, a series of pulse height determinations was made for each of several conditions. Two hundred pulse heights were measured for each of four conditions listed in Table 5-9.

Pulse repetition rate as a function of voltage across the power supply was determined. Table 5-1C shows the resultant data.

TABLE 5-8. STANDARD DEVIATION OF STROBE PULSE HEIGHT DISTRIBUTION

Strobe and Conditions	Standard Deviation (% of Arithmetic Mean)
*Whelen 1 (.24-m cable)	15%
*Whelen 1 (11.8-m cable)	3.8%
**Grimes G-260 (unfiltered detector)	2.5%
**Grimes G-260 (RG-780 filtered detector)	0.40%

*Operating at 24 VDC across power supply; unfiltered silicon photodiode detector.

**Operating at 14 VDC across power supply; .12-m connection; silicon photodiode detector.

TABLE 5-9. STANDARD DEVIATION OF STROBE PULSE HEIGHT DISTRIBUTIONS FOR STROBE SS-1

Conditions	Standard Deviation (% of Arithmetic Mean)
14 VDC; no filter, Si detector	3.9%
14 VDC; RG-780 filter, Si detector	2.4%
28 VDC; no filter	2.2%
28 VDC; RG-780 filter	3.1%

TABLE 5-10. STROBE PULSE REPETITION RATES

Power Supply	Pulse Repetition Rate		
	Power Supply @ 14 VDC	Power Supply @ 24 VDC	Power Supply @ 28 VDC
*Grimes 1	53 PPM		
**Whelen 1	"	80 PPM	80 PPM
**Whelen 2	"	59 PPM	59 PPM
**Whelen 3L	"	42 PPM	42 PPM
**Whelen 4	"	46 PPM	46 PPM
**Whelen 7L	"	47 PPM	47 PPM
Symbolic SS-1 Displays	46 PPM	49 PPM	49 PPM

*With each of 3 lamps.
**With each of 6 lamps.

6. SUMMARY

Aircraft xenon strobe lights have been developed to supplement or replace rotating beacons hitherto used for aircraft anticollision lights. Present specifications for these lights are stated in photometric units and take into account the visual response curve in the spectral region from 400 to 700 nanometers and include the integrating response of the eye to light pulses of short duration. These same lights have been considered for the cooperative portion of an Airborne Proximity Warning Indicator (APWI) system, making use of a silicon photodiode detector most sensitive in the near infrared region, between 800 and 1100 nanometers. The present report documents radiometric measurements made for the APWI Program Office at the Transportation Systems Center over a period of four years, on an assortment of aircraft xenon strobe lights selected to represent a cross-section of such strobes available to the flying community.

The peak radiant intensity of the Whelen Unit #7 (A470) with a Fresnel lens was approximately 2,000 watts per steradian in the 750 to 1,250-nm region of the spectrum. Unit #7 was used during the flight tests mentioned in Reference 5. It represents one half the intensity assumed in the original Leigh, Richardson analysis presented in Reference 4. This value appears to be a good average value for such units designed to meet the 400-candella requirement of the FAR's for anticollision lights. Taking into account factors such as aging of the lamp, cable length, and beam pattern variations, a conservative value would appear to be 1,000 watts/steradian for xenon lights of this type. Typical values of rise time and pulse duration for units with short cables are 30-μsec rise and 300-μsec duration. Deviations from these typical values are significant, and specific values should be obtained from the main body of the report. The measurements include spectral peak radiant intensity, spectral radiant energy, rise time duration, decay time versus wavelength, spectral analysis from 0 to 190 kHz, radiant geometry, photometric calibration, and strobe stability.

REFERENCES

1. Carlson, N.A., Grundy, P.A., Morth, H.R., Copps, E.M. and Flanders, J.H., "PWI Test and Developmental Resource Utilization - Final Report," Intermetrics, Inc., 15 November 1971.

2. Davidson, G.A. and Hardy, A.C., "On the Perception of Flashes of Light at the Limit of their Perceptibility," Massachusetts Institute of Technology, Instrumentation Laboratory Report E-1492, 1964.

3. Edgerton, H.E. and Killian, J.R. "Flash," Branford Press, 1954.

4. Leigh, Charles H. and Richardson, Albert S. Jr., "Performance Analysis of an Infrared Pilot Warning System," Proceedings of the IEEE, Vol. 58, March 1970.

5. Phillips, Charles O. Jr. et al., "Flight Test Evaluation and Analysis of an Optical IR PWI System," Report DOT-TSC-NASA-72-1, 1972.